Endogenous corazonin signaling modulates the post-mating switch in behavior and physiology in females of the brown planthopper and *Drosophila*

Ning Zhang (张宁)[1], Shao-Cong Su (苏少聪)[1], Ruo-Tong Bu (卜若彤)[1], Yi-Jie Zhang (张伊杰)[1], Lei Yang (杨磊)[1], Jie Chen (陈洁)[1], Dick R. Nässel[2], Cong-Fen Gao (高聪芬)[1], Shun-Fan Wu (吴顺凡)[1*]

Orcid ID numbers of Shun-Fan Wu: 0000-0003-0096-147X

Orcid ID numbers of Dick Nässel: 0000-0002-1147-7766

Affiliations:

[1]State Key Laboratory of Agricultural and Forestry Biosecurity, College of Plant Protection, Nanjing Agricultural University, Nanjing 210095, China

[2]Department of Zoology, Stockholm University, Stockholm, Sweden

[*]Correspondence: wusf@njau.edu.cn (S.F. Wu).

Abstract

Mating in insects commonly induces an alteration in behavior and physiology in the female that ensures optimal offspring. This is referred to as a post-mating response (PMR). The induction of a PMR requires not only male-derived factors transferred with semen during copulation, such as sex peptide (SP) in *Drosophila*, but also intrinsic female signaling components. The latter signaling remains poorly understood in most insects, including the brown planthopper (BPH) *Nilaparvata lugens*, a devastating rice pest. In BPHs the PMR comprises a reduced receptivity to re-mating and increased oviposition. Here, we demonstrate that the neuropeptide corazonin (CRZ) and its receptor (CrzR) are critical for the PMR in female BPHs. Peptide injection and knockdown of CRZ expression by RNAi or CRISPR/Cas9-mediated mutagenesis demonstrate that distensible CRZ signaling suppresses mating receptivity in virgin *N. lugens* females and mediates a reduction in re-mating frequency and increased ovulation. The *CrzR* is highly expressed in the female reproductive tract, and *CrzR*-knockdown phenocopies *Crz* diminishment. Importantly, female *CRZ/CrzR* signaling is indispensable for male seminal fluid factors (e.g. maccessin) to induce the PMR. With disrupted *CrzR* signaling, seminal fluid or maccessin injection fails to reduce female receptivity. Notably, CRZ is not produced in male accessory gland (MAG) and thus not transferred during copulation. However, male *Crz* knockout impairs the PMR in mated females and combining male and female *Crz* knockouts nearly abolished the PMR, demonstrating that CRZ is essential for PMR generation. Transcriptomics of the MAG indicates that *Crz* knockout affects the expression of numerous seminal fluid protein genes. Finally, we found that also in female *Drosophila melanogaster*, disrupted *Crz* signaling resulted in increased re-mating and reduced oviposition, while CRZ injection suppressed virgin receptivity and increased oviposition. In summary, our study reveals that endogenous female CRZ signaling and male-derived signals cooperate to regulate post-mating transitions in BPHs and *Drosophila*.

Keywords: Post mating response; *Nilaparvara lugens*; *Drosophila melanogaster*; corazonin; corazonin receptor

Introduction

Reproductive behavior is critical for population sustenance and survival of species, and is influenced by a complex array of internal conditions, environmental factors, and social interactions. In insects, males typically initiate mating through courtship, while females determine acceptance by integrating external sensory stimuli with their internal state. Consequently, female reproductive activity is modulated by multiple signaling pathways[1-8]. In insects, successful copulation commonly induces profound physiological and behavioral changes in the females [5,9-18].

Following their first mating, insect females typically reject further courtship attempts and initiate oviposition. This distinct shift in behavior and physiology is referred to as a post-mating response (PMR) [5-7,19-23]. A PMR has been documented across diverse insect taxa, including *Drosophila melanogaster*, *Anopheles gambiae, Aedes aegypti* and the brown planthopper (BPH), *Nilaparvata lugens* [6,18,21,24,25].

Induction of a PMR commonly requires the transfer of specific seminal fluid components during copulation. In *Drosophila*, seminal fluid peptides, including sex peptide (SP) and DUP99B produced in male accessory glands (MAG), enter the female reproductive tract, bind to specific receptors on sensory neurons, and activate signaling pathways that drive post-mating behavior and physiology [6,13,14,18,26]. Additional factors such as Acp26Ab and ovulin (Acp26Aa) are also transferred with the seminal fluid and modulate female reproductive physiology in *Drosophila* [27-30]. Notably, it has been shown that the PMR-inducing substances, produced in the MAG

of various insects, are highly species-specific and not even conserved across related taxonomic groups [25,31].

While MAG-derived sex peptide (SP) and its receptor (SPR) are key regulators of the female post-mating response (PMR) in *Drosophila* [5-7,16], additional signaling pathways intrinsic to females also modulate this process. Interneurons within abdominal neuromeres of the ventral nerve cord (VNC) promote receptivity to males by signaling via myoinhibitory peptide (MIP) to brain circuits [32]. Furthermore, the neuropeptide diuretic hormone 44 (DH44) modulates female sexual receptivity through a sex-specific brain circuit; mating suppresses DH44 signaling, thereby reducing receptivity [1]. During sexual maturation, leucokinin (LK)-expressing neurons (ABLKs) in the abdominal ganglion, downstream of SP-activated circuitry, suppress female receptivity [33]. In addition to changes in receptivity, the *Drosophila* PMR includes a shift in diet preference toward yeast consumption. This altered feeding behavior is mediated by specific peptidergic neurons (ALKs) in the brain through LK signaling [12].

Although the mechanisms and neuronal pathways underlying the post-mating response (PMR) in *Drosophila* are well characterized [3,4,6,7,34-37], this process remains poorly understood in most non-model insects. A prominent example is the brown planthopper (BPH), *N. lugens* (Hemiptera). As a monophagous rice pest, the BPH exhibits robust reproductive capacity and remarkable environmental adaptability [38]. It has also developed high resistance to diverse chemical pesticides [39-41]. Consequently,

elucidating reproductive physiology and behavior in BPHs is crucial for developing novel control strategies.

In BPHs, the recently identified MAG-derived peptide maccessin (macc) is transferred during copulation and triggers a PMR in females, although its receptor remains unknown [25]. Notably, the same study demonstrated that a second peptide, ion transport-like peptide 1 (ITPL-1), also modulates the PMR. Whereas macc is male-specific, ITPL-1 is produced both in the MAG and endogenously in females, where it reduces female receptivity to courting males [25]. Given its endogenous female expression, ITPL-1 likely functions as an intrinsic signaling component in the PMR of BPHs, analogous to the role of myoinhibitory peptide (MIP) and DH44 in *Drosophila* females [1,32].

Here, we explored the role of another neuropeptide, corazonin (CRZ), in the reproductive behavior of BPHs. In *Drosophila* males, CRZ is released from interneurons of the ventral nerve cord (VNC) and acts on serotonergic projection neurons to regulate ejaculation and copulation duration [42]. Additionally, CRZ release in males during mating mitigates mating-induced heart rate acceleration, to promote physiological recovery [43]. CRZ furthermore influences post-mating dietary preference in males [12]. Surprisingly, the role of CRZ signaling in female reproduction remains unexplored. To fill this gap, we examined the role of CRZ in female reproduction, including the PMR, in BPH and *Drosophila melanogaster*.

In this study, we demonstrate that CRZ induces a post-mating switch in receptivity in females of both BPH and *Drosophila*. Notably, CRZ injection in virgin females

diminishes receptivity to courting males, while *Crz* knockdown or knockout in mated females renders them receptive to further mating. Importantly, CRZ is not produced in the MAG, and thus not transferred from males, but acts as an endogenously produced peptide in females. Furthermore, we detected strong expression of the CRZ receptor (*CrzR*) in the female reproductive tract of BPHs. We demonstrated that both CRISPR-Cas9-mediated *CrzR* knockout and RNAi-mediated *CrzR* knockdown disrupt the PMR, phenocopying *Crz* knockdown. Critically, we could show that the level of receptivity to mating in virgin females, whether by MAG extract (with seminal fluid proteins) injection or macc injection, is strictly dependent on presence of the *CrzR* receptor. Importantly, manipulations of CRZ signaling in female *Drosophila* yield similar effects on receptivity and oviposition. Interestingly, we find that knockdown or knockout of *Crz* in male *N. lugens* does not affect male copulation behavior, but *Crz* deficient males do not induce a full PMR in mated females. Notably, knockout of *Crz* in both male and female partners results in an almost complete abolishment of the PMR. Since CRZ is not produced in the MAG we performed a transcriptomic analysis of the MAG in *Crz* mutants to screen for other candidate CRZ-regulated genes affecting the PMR. We found altered expression of a large number of genes, containing seminal protein genes, but no change in the genes encoding *macc* and *ITPL-1*, suggesting presence of other MAG factors, yet to be identified. In summary, our findings strengthen the notion that the female PMR requires not only transfer of male-derived factors, but also endogenous female neuropeptide signaling components.

Results

CRZ signaling reduces receptivity to courting males and stimulates oviposition in *N. lugens* females

While numerous studies have established roles of the neuropeptide CRZ in regulating aspects of male reproduction across diverse insect species [44-50], research addressing its potential functions in female reproduction remains conspicuously lacking.

This study investigates the role of CRZ in female reproduction, starting with the brown planthopper (BPH), *Nilaparvata lugens*, a major agricultural pest. Initially, the *Crz* gene (GenBank accession: AB817247.1) was cloned based on transcriptome data [51]. The deduced mature CRZ sequence in BPH, pQTFQYSRGWTNamide, is identical to that reported for most studied insect species (Figure 1-figure supplement 1A). Consistent with other known CRZ precursors, the BPH precursor encodes a single CRZ peptide starting at the first amino acid of the propeptide (Figure 1-figure supplement 1A and B). A comparison of the organization of selected CRZ precursor genes is shown in Figure 1-figure supplement 1B. Genomic analysis revealed that the CRZ precursor is encoded by two exons separated by a single intron (Figure 1-figure supplement 1B). The mature CRZ peptide and a scrambled control peptide (sCRZ) were synthesized for pharmacological experiments.

First, we investigated the role of CRZ signaling in the reproductive behavior and PMR of female BPHs. The PMR in BPHs, is characterized by reduced receptivity to courting males, including display of rejection behaviors, and increased oviposition [25].

This response is partially induced by the male-derived peptide maccessin (macc), transferred during copulation [25]. We found that injection of CRZ significantly reduced receptivity of virgin female BPHs to courting males (Figure 1A and B). Furthermore, virgin females injected with CRZ actively rejected courting males, exhibiting a distinct rejection behavior characterized by ovipositor extrusion and kicking or fleeing. This behavior was not observed in control females injected with sCRZ (Figure 1 Supplementary Video 1). Notably, the CRZ-induced mating refusal behavior in virgin females was no longer observed 24 hours after injection (Figure 1-figure supplement 2A). While injection of CRZ peptide did not stimulate egg production in virgin BPHs (Figure 1-figure supplement 2B), it significantly promoted oviposition in mated females (Figure 1C).

To further investigate CRZ action, we performed RNA interference (RNAi) by injecting double-stranded *Crz* RNA (*dsNlcrz*) into female BPHs, which efficiently reduced *Crz* expression (Figure 1-figure supplement 2). Knockdown of *Crz* resulted in increased receptivity with 10% of the mated females mating again, and significantly reduced oviposition to approximately 60% of control levels (Figure 1E and F). In contrast, *Crz* knockdown had no effect on the receptivity of virgin females (Figure 1E).

Since RNAi-mediated knockdown of *Crz* in female BPHs left a residual level of gene expression (Figure 1-figure supplement 2), we generated two *Crz* deletion alleles, ΔCrz^1 and ΔCrz^2, using CRISPR/Cas9 (Figure 1G-G') to achieve a complete ablation. Both alleles harbor deletions eliminating the mature CRZ peptide coding sequence (Figure 1G''). Sanger sequencing confirmed that the deletions

compromised essential triplet codons within the *Crz* open reading frame (Figure 1-figure supplement 4), thereby efficiently disrupting CRZ peptide expression (Figure 1G'' and H). Immunohistochemical analysis further validated the mutants, revealing a complete absence of anti-CRZ immunolabeling in homozygous ΔCrz^1 and ΔCrz^2 females (Figure 1H). Homozygous ΔCrz^1 and ΔCrz^2 virgin females are fully viable and fertile. They exhibit a courtship vigor similar to controls and their initial mating success rate with wild-type males exceeds 60% (Figure 1I and J). However, 25% of the mated mutant females were receptive to further mating (Figure 1J), and oviposition was significantly reduced to approximately 50% of the wild-type levels (Figure 1K). Collectively, these results demonstrate that diminished CRZ signaling severely perturbs the PMR in female BPHs, seen as increased post-mating receptivity and reduced egg-laying. Importantly, the *Crz* deletion abolished the onset of typical post-mating rejection behavior. We, thus, conclude that endogenous CRZ signaling is important for the induction of a PMR in female BPHs.

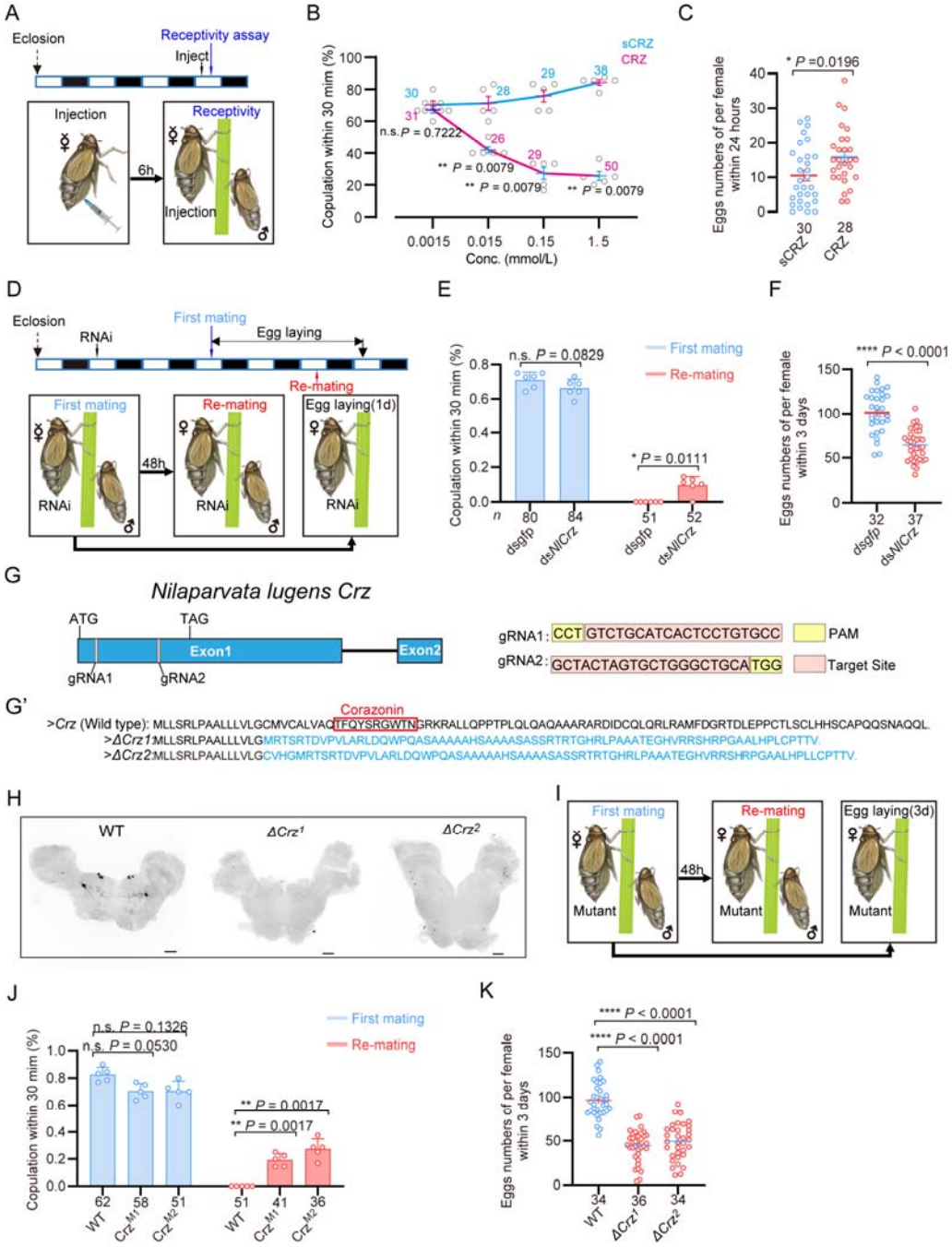

Figure 1. CRZ signaling affects the post-mating response (PMR) and oviposition in female *N. lugens*.

Wild-type males were used in all behavioral assays.

(A) Experimental design for panels B-C. The white/black segments on the experimental time lines denote light/dark periods, respectively.

(B) Receptivity of virgin females 6 h post-injection, using different doses of CRZ (sCRZ as

control), each virgin female BPH was injected with a calibrated glass capillary needle directly into the abdomen with 100 ng/10 ng/1 ng/0.1 ng of peptide dissolved in 50 nL of 1 × PBS balanced salt solution. The graph shows percentage females copulating within 30 min. ***P* < 0.01 vs. control; ns (non-significant): *P* > 0.05 (Mann-Whitney test). The numbers above the curves denote total number of animals.

(C) Eggs laid per mated female 12 h post-copulation. We used the highest CRZ dose from panel B (sCRZ, control). Each mated female BPH was injected with a calibrated glass capillary needle directly into the abdomen with 100 ng of peptide dissolved in 50 nL of 1 × PBS balanced salt solution. **P* < 0.05 (Student's t-test). Data: mean ± s.e.m (≥3 biological replicates, ≥8 insects/replicate). The numbers below the bars denote total number of animals.

(D) Experimental design for panels E-F.

(E) Receptivity of virgin (1st mating) and mated females after *Crz*-RNAi (*dsgfp* as control). Graph displays the percentage of females copulating within 30 min. The small circles denote the number of replicates; the numbers below the bars denote total number of animals. Data are shown as mean ± s.e.m. *P < 0.05, and ns (non-significant), *P* > 0.05, two-way ANOVA followed by Holm-Šídák's multiple comparisons test.

(F) Total numbers of eggs laid per female over 72 h after *Crz*-RNAi (*dsgfp* as control). ****P* < 0.0001 (Student's *t*-test). The small circles and the numbers below the bars denote total number of animals. Data are shown as mean ± s.e.m. (≥3 biological replicates, ≥8 insects/replicate).

(G) Schematic diagram of the *Crz* gene and sgRNA (single-guide RNA) design for *Crz* mutant production. The *Crz* gene consists of 2 exons, and ATG and TAG are located on Exon 1. The target site of the 20 bp sgRNA on Exon 1 is highlighted in pink. The PAM sites are indicated in yellow. The two knockout strains ΔCrz^1 and ΔCrz^2 were unable to produce mature CRZ peptides. (G') The amino acid sequences obtained by translating the mutated base sequences.

(H) Absence of CRZ immunoreactivity in homozygous ΔCrz^1 and ΔCrz^2 mutants compared to wild type (WT) expression. Scale bars: 50 μm.

(I) Experimental design for panels J-K.

(J) Receptivity of virgin/mated females across genotypes. No effect was seen on virgin receptivity, only the re-mating was affected. The small circles denote the number of replicates; the numbers below the bars denote total number of animals. Data are shown as mean ± s.e.m. ***P* < 0.01; ****P* < 0.001, and ns (non-significant), *P* > 0.05, two-way ANOVA followed by Holm-Šídák's multiple comparisons test.

(K) Eggs laid 72 h post-mating. The numbers below the bars denote total number of animals. Data are shown as mean ± s.e.m. *****P* < 0.0001; Student's *t* test.

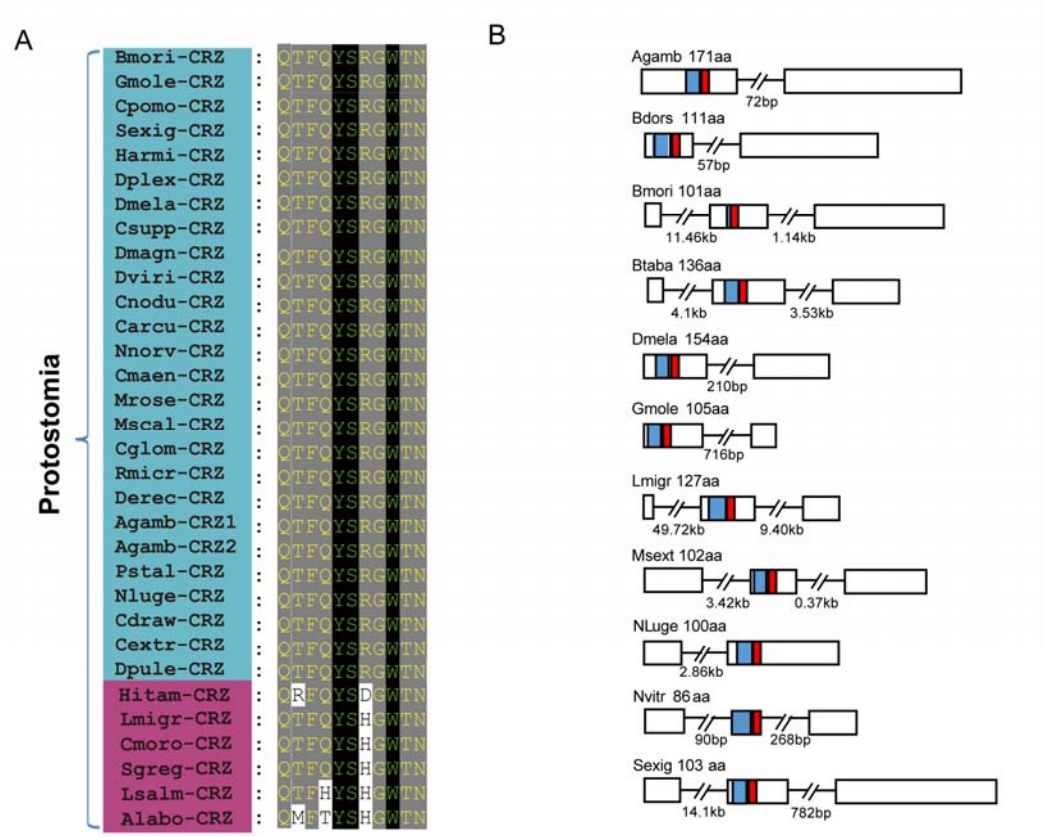

Figure 1 - figure supplement 1. Evolutionary conservation of CRZ peptide sequences in *Nilaparvata lugens* and other arthropods.

(A) Alignment of mature CRZ peptide sequences across species.

Abbreviations of species names are as follows: Bmori (*Bombyx mori*), Gmole (*Grapholita molesta*), Cpomo (*Cydia pomonella*), Sexig (*Spodoptera exigua*), Harmi (*Helicoverpa armigera*), Dplex (*Danaus plexippus*), Dmela (*Drosophila melanogaster*), Csupp (*Chilo suppressalis*), Dmagn (*Daphnia magan*), Dviri (*Drosophila virilis*), Cnodu *(Catagly nodus*), Carcu (*Callinectes arcuatus*), Nnorv (*Nephrops norvegicus*), Cmaen (*Carcinus maenas*), Mrose (*Macrobrachium rosenbergii*), Mscal (*Megaselia scalaris*), Cglom (*Cotesia glomerata*), Rmicr (*Rhipicephalus microplus*), Derec (*Drosophila erecta*), Agamb (*Anopheles gambiae*), Pstal (*Plautia stali*), Nluge (*Nilaparvata lugens*), Cdraw (*Caerostris darvini*), Cextr (*Caerostris extrusa*), Dpule (*Daphnia pulex*), Hitam (*Heterotrigona itama*), Lmigr (*Locusta migratoria*), Cmoro (*Carausius morosus*), Sgreg (*Schistocerca gregaria*), Lsalm (*Lepeophtheirus salmonis*), Alabo (*Apis laboriosa*). Species within the blue area possess highly conserved mature peptide sequences, whereas those in the magenta zone exhibit relatively less conservation in their mature peptides.

(B) Schematic organization of CRZ precursors in representative species. Signal peptides (blue) and mature CRZ peptides (red) are indicated.

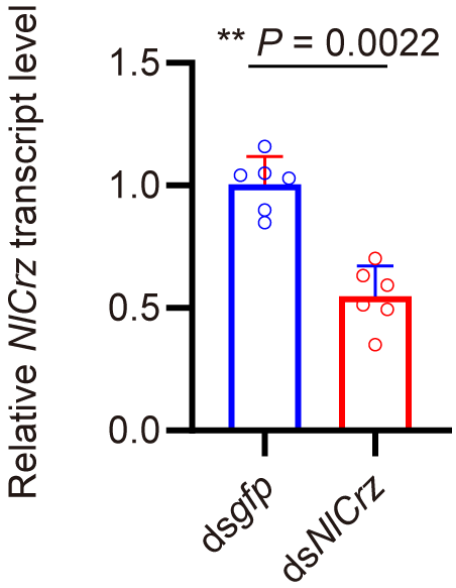

Figure 1 - figure supplement 2. The *Crz* gene-silencing efficacy in female insects following dsRNA injection assayed by qPCR. The small circles denote the number of replicates. Data are shown as mean ± s.e.m. Mann–Whitney test. ***P<0.001.

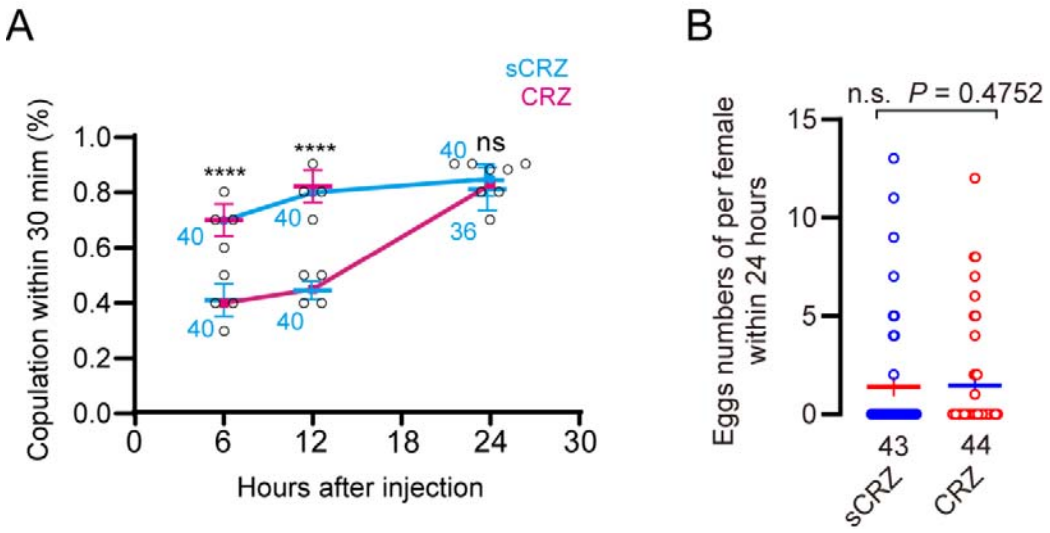

Figure 1 - figure supplement 3. Phenotypic effects of CRZ peptide injection and *Crz* gene knockout.

(A) Receptivity of virgin females at indicated time points after CRZ injection (sCRZ as control). Each virgin female BPH was injected with a calibrated glass capillary needle directly into the abdomen with 100 ng of peptide dissolved in 50 nL of 1 × PBS balanced salt solution. Graph shows percentage females copulating within 30 min. ****P < 0.0001; ns: not significant (Chi-square test). The numbers associated with the curves denote total number of animals.

(B) Eggs laid per virgin female after neuropeptide injection (sCRZ, control). Females were mated with wild-type males for 12 h prior to assessment. Each virgin female BPH was injected with a calibrated glass capillary needle directly into the abdomen with 100 ng of peptide dissolved in 50 nL of 1 × PBS balanced salt solution. Data are shown as mean ± s.e.m. ns: P > 0.05 (Student's t-test). The numbers below the bars denote total number of animals. We used at least four biological replicates with at least ten insects per replicate for each experiment.

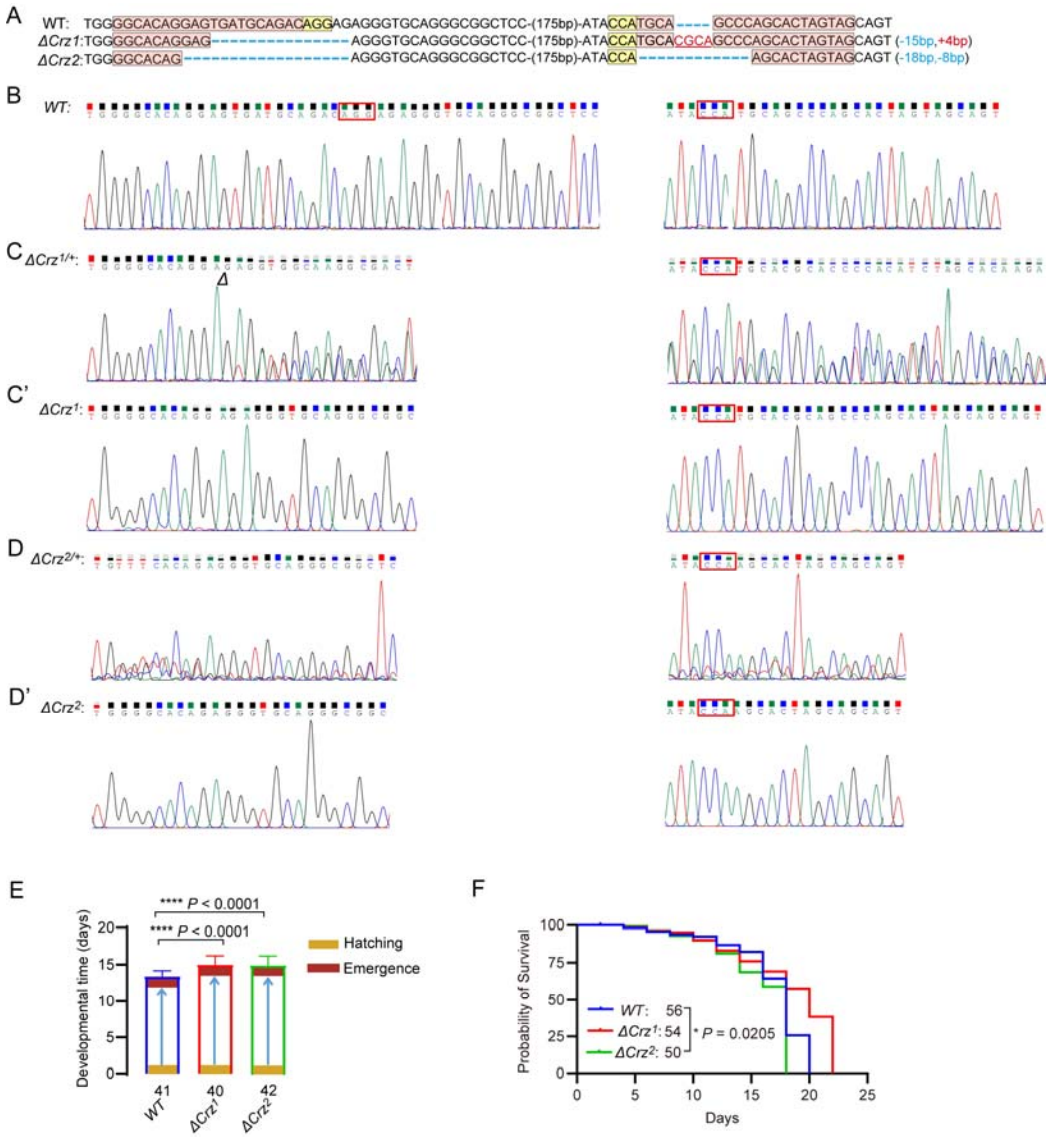

Figure 1 - figure supplement 4. Characterization of *Crz* mutants in *N. lugens*.

(A) Sequencing of *Crz* mutant (*ΔCrz*^{1} and *ΔCrz*^{2}) and wild type (WT) PCR products from BPHs. The exact indel types of the G0 mutant individuals were confirmed by cloning and sequencing. The wild-type sequences are shown at the top with the target site marked by in pink shading and PAM in yellow shading. The change in the length of the mutant sequence is shown on the right side of the sequence (+, insertion; -, deletion). (B) The Sanger sequence chromatograms flanking the sgRNA target site for wild type (WT). (C and D) The Sanger sequence chromatograms flanking the sgRNA target site for wild type (WT), heterozygous mutant (*ΔCrz*$^{1/+}$ and *ΔCrz*$^{2/+}$). (C' and D') The Sanger sequence chromatograms flanking the sgRNA target site for wild type (WT), homozygous mutant (*ΔCrz*^{1} and *ΔCrz*^{2}).

(E) Developmental duration (egg to adult) across genotypes. ****P < 0.0001 (Student's *t*-test). The numbers below the bars denote total number of animals. (F) Survival curves of adult *Crz* mutants vs. WT. *P < 0.05 (Log-rank Mantel-Cox test; df = 1; n ≥ 50/group).

CRZ is expressed in similar neurons in both sexes of BPHs and is absent from the male accessory gland

To further understand how CRZ regulates the PMR in BPHs, we examined the expression of CRZ and *Crz* across different tissues in males and females. The *Crz* mRNA expression was examined in various BPH tissues using both RT-PCR and qPCR (Figure 2A). We detected *Crz* mRNA expression primarily in the central nervous system (CNS), regardless of the primer set or detection method used, while expression was nearly undetectable in other tissues, including reproductive organs of both sexes (Figure 2B and C).

A previous study reported CRZ expression in four male-specific interneurons within the abdominal ganglia of *Drosophila* [44]. To determine whether CRZ exhibits sexually dimorphic expression in BPHs, we performed immunolabeling using an anti-CRZ antiserum. This labeled four pairs of neurons in the protocerebrum of the brain (Figure 2D and E) and one pair of neurons in the subesophageal ganglion in both males and females (Figure 2D and E). Since CRZ immunolabeled neurons in brains of most, if not all, insects studied include three or more pairs of lateral neurosecretory cells [52,53], we suggest that CRZ signaling regulating the PMR may be hormonal (at least in part). Importantly, no CRZ-immunopositive neurons were detected in the abdominal ganglia of either sex (Figure 2D and E), and thus there is no evidence for sex-specific expression of CRZ neurons in BPHs. This is in contrast to *Drosophila*, where we confirmed, as previously reported [42], the presence of CRZ-immunolabeled neurons specifically in the abdominal ganglia of males (Figure 2

- figure supplement 1A).

To exclude that CRZ acts as a seminal fluid peptide transferred to females during copulation, similar to sex peptide (SP) in *Drosophila* and macc in BPHs [25], we specifically examined CRZ expression in reproductive tissues of both sexes. However, we observed no CRZ immunolabeling in the male reproductive organs (Figure 2 - figure supplement 1B1 - B3) or female reproductive organs (Figure 2 - figure supplement 1B4 – B6). This aligns with our transcriptional *Crz* data shown above (Figure 2B and C). Furthermore, *Crz* mRNA and CRZ protein were absent from transcriptomic and proteomic datasets of the male accessory glands (MAGs) in BPHs [25]. Collectively the available data suggest, that CRZ is not produced by the MAG and is consequently unlikely to be transferred to females as a seminal fluid component.

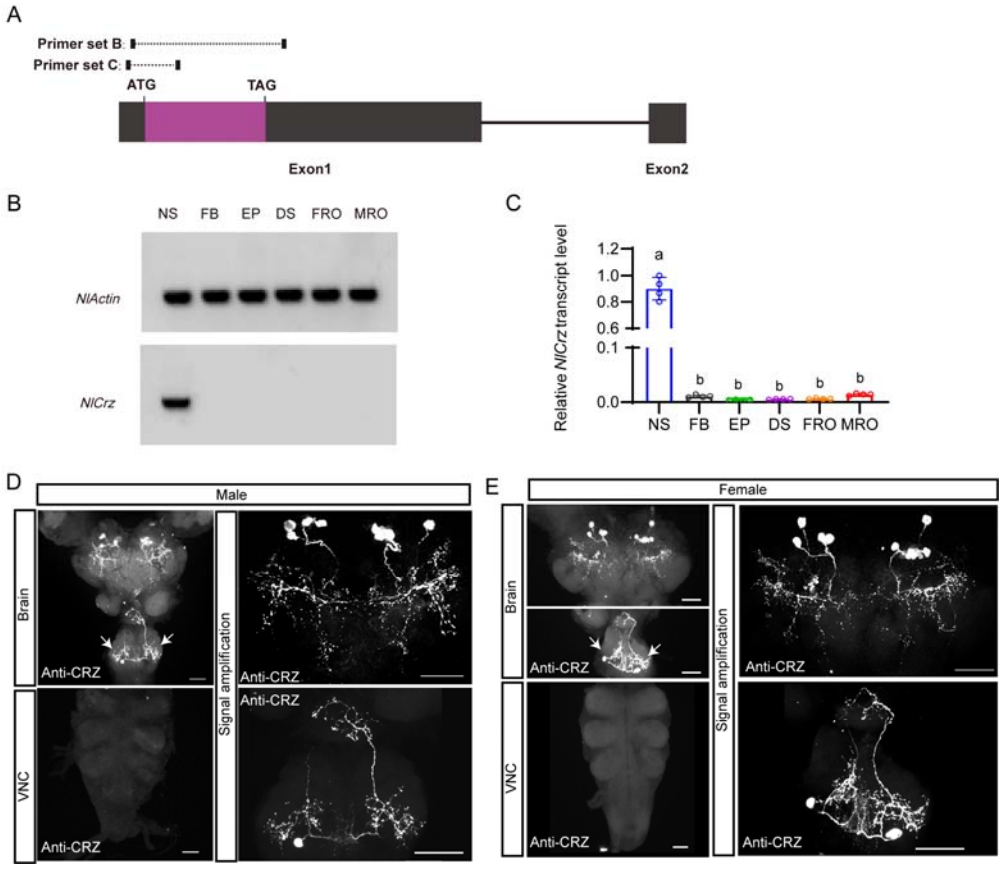

Figure 2. Expression of *Crz* and CRZ in the nervous system of the brown planthopper (BPH). (A) Schematic of primer design for *Crz* detection (primer sequences provided in Table S1). (B) RT-PCR analysis of *Crz* mRNA levels in various BPH tissues. Actin served as the loading control. Tissues: Nervous system (NS), fat body (FB), Epidermis (EP), digestive system (DS), female reproductive organs (FRO), male reproductive organs (MRO). Note: Tissues except reproductive organs were pooled from both sexes.

(C) qPCR analysis of *Crz* mRNA levels in BPH tissues (abbreviations as in B).

(D and E) Immunolocalization of CRZ peptide in the nervous system of male (D) and female (E) BPHs. Four pairs of CRZ neurons in the brain and one pair in the subesophageal ganglion are shown. Note that some of the CRZ neurons are likely to be neurosecretory cells with terminations in the corpora cardiaca, others may be interneurons. The extensive branches within the brain suggest CRZ signaling in brain circuits. VNC, ventral nerve cord. Scale bars: 50 µm. (E) CRZ immunolabeling in the nervous system of female BPHs. Scale bar: 50 µm.

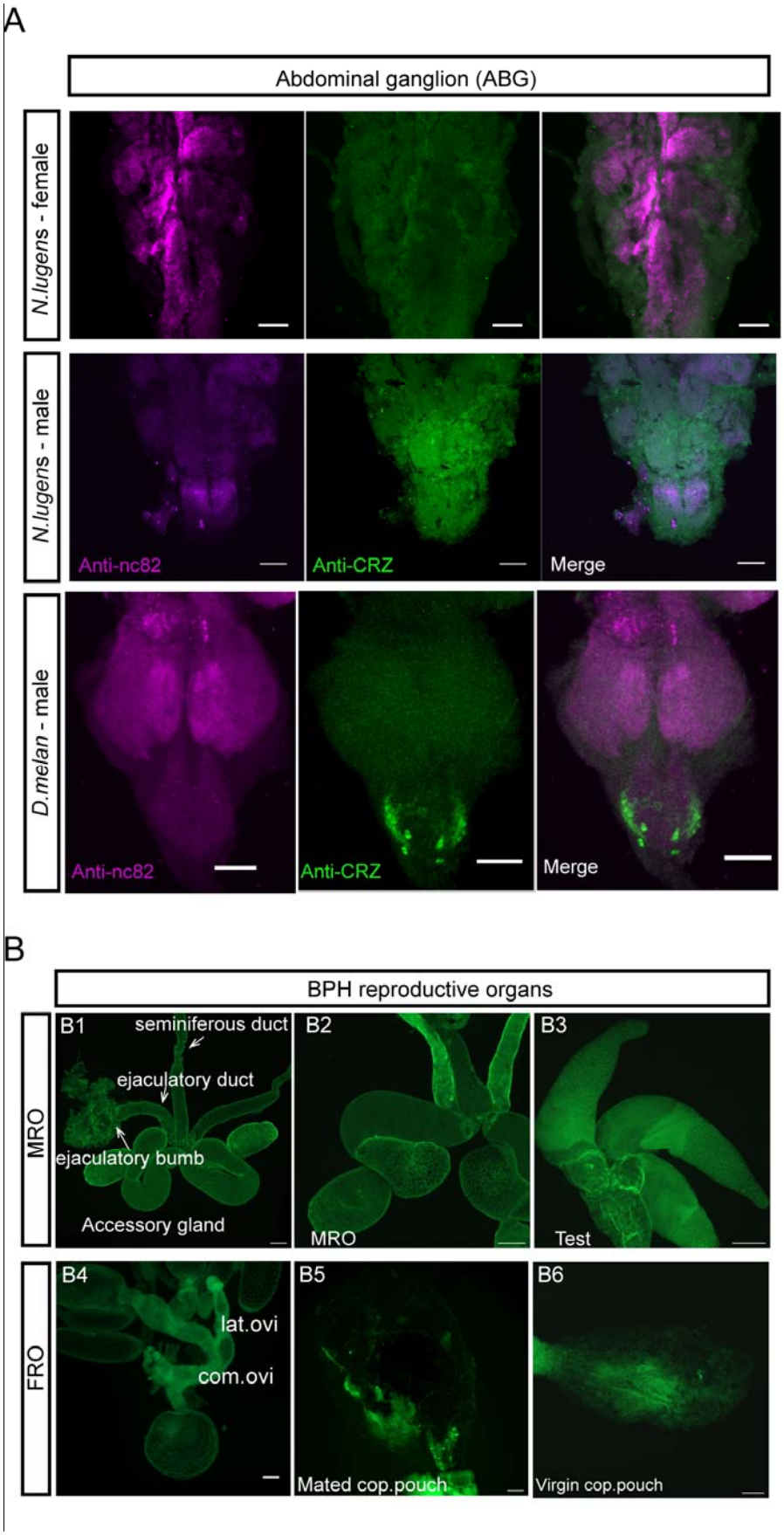
A
Abdominal ganglion (ABG)
N.lugens - female
N.lugens - male
D.melan - male
Anti-nc82
Anti-CRZ
Merge
B
BPH reproductive organs
MRO
FRO
B1
seminiferous duct
ejaculatory duct
ejaculatory bumb
Accessory gland
B2
MRO
B3
Test
B4
lat.ovi
com.ovi
B5
Mated cop.pouch
B6
Virgin cop.pouch

338

Figure 2 - figure supplement 1. CRZ immunolabeling in abdominal ganglion and reproductive organs of male and female BPHs.

(A) Anti-CRZ immunolabeling in the abdominal ganglia of the ventral nerve cord (VNC) in *N. lugens* and *Drosophila melanogaster* (*D. Melan.*). Scale bar: 50 μm. Note: Male-specific CRZ-positive neurons are present in *D. melanogaster*, as previously reported.

(B) Lack of CRZ immunoreactivity in BPH reproductive organs. (B1-B3) Male reproductive organs (MRO): testes (test). (B4-B6) Female reproductive organs (FRO): lateral oviduct (Lat. ov), common oviduct (Com. ov). Scale bars: 100 μm.

The CRZ receptor is essential for mediating the post mating response in female BPHs

Given our findings implicating CRZ in modulating the PMR in female BPHs, we identified the CRZ receptor (*CrzR*) gene in this species; it encodes a structurally conserved GPCR orthologous to other insect *CrzR*s (Figure 3-supplemental figure 1). We next explored the effect of knocking down the *CrzR* on the PMR in BPHs. RNAi-mediated knockdown of the receptor (*dsCrzR* injection) resulted in 15% of the mated females re-mating, a phenotype not seen in *dsgfp*-injected controls (Figure 3A and B) and in a significantly reduced oviposition (Figure 3C). Importantly, CRZ injection failed to diminish receptivity in *CrzR*-knockdown virgins (Figure 3D and E). Furthermore, MAG extract (with seminal fluid proteins) injection into *dsCrzR*-treated virgins did not affect receptivity (Figure 3F).

To further confirm the role of the *CrzR* in the PMR of BPHs, we applied CRISPR/Cas9 genome editing to mutate the *CrzR* gene and constructed a homozygous mutant strain of *CrzR* ($CrzR^M$) by genetic crosses (Figure 3G-3G'', Fig. 3 - figure supplement 2A). We found that the developmental time and life span of the female *CrzR* mutants, like the *Crz* mutants, were slightly extended compared to wild type animals (Figure 3 - supplement figure 2D and 2E). Homozygous $CrzR^M$ females displayed increased remating rates (30%) (Figure 3I and J) and the number of eggs laid by $CrzR^M$ females was also significantly decreased (Figure 3K). Consistent with the RNAi results, neither CRZ nor MAG extract injections reduced receptivity in $CrzR^M$ virgins (Figure 3K - M). Finally, macc peptide injection also failed to decrease

receptivity in *CrzR*-mutant virgins (70% acceptance rate), whereas it significantly suppressed mating in wild-type controls (Figure 3N). These results collectively demonstrate that intact CRZ/CrzR signaling in female BPHs is required for transducing the PMR-inducing effects of male-derived seminal factors, including macc [25].

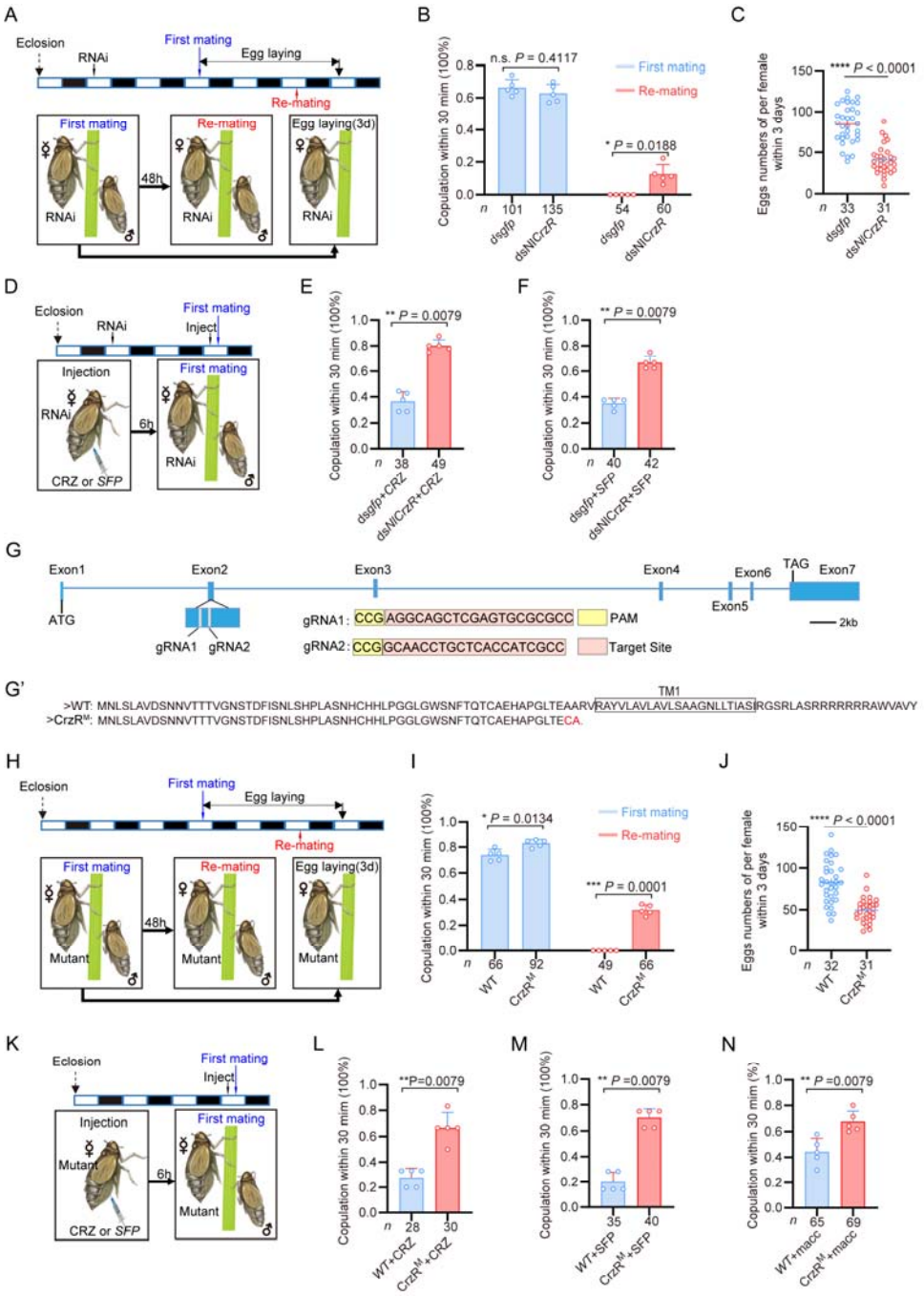

Figure 3. The CRZ receptor (*CrzR*) is essential for the female PMR and is required for action of MAG-derived factors**.**

(A) Experimental design for B and C.

(B) Receptivity after *CrzR*-RNAi (injection of ds*CrzR*; ds*GFP* as control). Percentage females copulating within 30 min. The small circles denote the number of replicates; the numbers below the bars denote total number of animals. Data are shown as mean ± s.e.m. *$P < 0.05$,

and ns (non-significant), $P > 0.05$, two-way ANOVA followed by Holm-Šídák's multiple comparisons test.

(C) Numbers of eggs laid within 72 h post-mating (*dsCrzR* females × WT males). Data are shown as mean ± s.e.m. ****$P < 0.0001$ (Student's *t*-test). The numbers below the bars denote total number of animals.

(D) Experimental design for E-F.

(E) Receptivity after CRZ injection in *CrzR*-knockdown virgins (*dsGFP* + CRZ control). Graph shows percentage females copulating within 30 min. Each virgin female BPH was injected with a calibrated glass capillary needle directly into the abdomen with 10 ng of peptide dissolved in 50 nL of 1 × PBS balanced salt solution. The small circles denote the number of replicates; the numbers below the bars denote total number of animals. Data are shown as mean ± s.e.m. **$P < 0.01$ (Mann-Whitney test).

(F) Receptivity after MAG extract (with seminal fluid proteins) injection in *CrzR*-knockdown virgins (*dsGFP* + SFP control). Percentage copulating within 30 min. The small circles denote the number of replicates; the numbers below the bars denote total number of animals. Data are shown as mean ± s.e.m. **$P < 0.01$ (Mann-Whitney test).

(G) *CrzR* targeting strategy for generation of mutants. *Top:* Genomic structure (ATG/TAG in Exons 2/7). sgRNA target (pink), PAM (yellow). *Bottom:* CRISPR alleles.

(G') Translated receptor mutant sequences.

(H) Experimental design for I-J.

(I) Receptivity of *CrzR* mutants compared to wild type animals (WT). The small circles denote the number of replicates; the numbers below the bars denote total number of animals. Data are shown as mean ± s.e.m. *$P < 0.05$, ***$P < 0.001$, two-way ANOVA followed by Holm-Šídák's multiple comparisons test.

(J) Number of eggs laid by mutants mated with WT males within 72 h. The numbers below the bars denote total number of animals. Data are shown as mean ± s.e.m. ****$P < 0.0001$; Student's *t* test.

(K) Experimental design for L-M.

(L) Receptivity after CRZ injection in *CrzR* mutants compared to WT. Each virgin female BPH was injected with a calibrated glass capillary needle directly into the abdomen with 10 ng of peptide dissolved in 50 nL of 1 × PBS balanced salt solution. The small circles denote the number of replicates; the numbers below the bars denote total number of animals. Data are shown as mean ± s.e.m. **$P < 0.01$, Mann–Whitney test.

(M) Receptivity after SFP injection in *CrzR* mutants compared to WT. The small circles denote the number of replicates; the numbers below the bars denote total number of animals. Data are shown as mean ± s.e.m. **$P < 0.01$, Mann–Whitney test.

(N) Receptivity after macc injection in *CrzR* mutants compared to WT. The small circles denote the number of replicates; the numbers below the bars denote total number of animals. Data are shown as mean ± s.e.m. **$P < 0.01$, Mann–Whitney test.

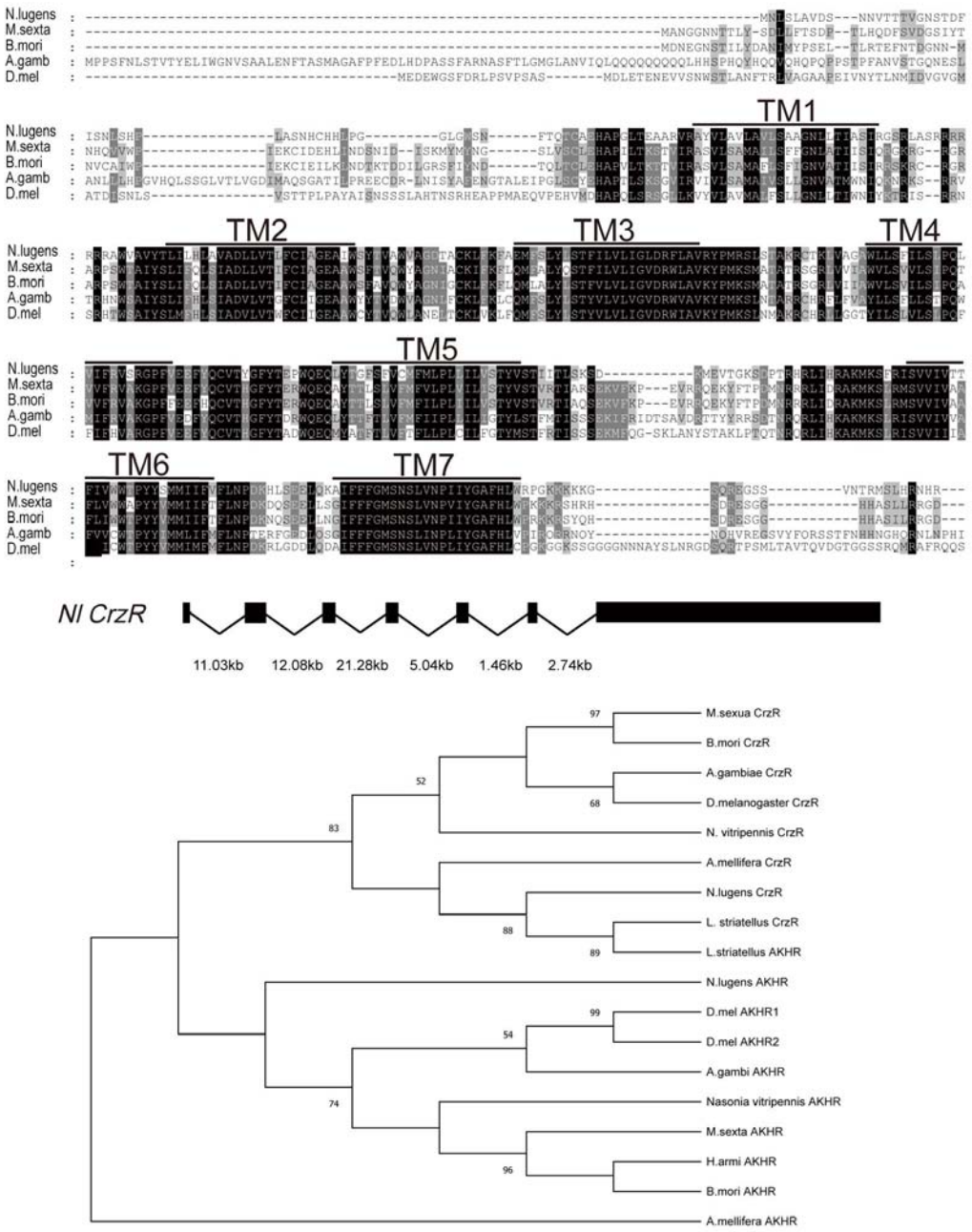

Figure 3 - figure supplement 1. Structural conservation of the *CrzR* across insect species. (A) Multiple sequence alignment highlighting conserved transmembrane domains (TM1-TM7, shaded) in CRZ receptor orthologs. The species shown are: *N. lugens*: *Nilaparvata lugens; M. sexta: Manduca sexta; B. mori*: *Bombyx mori*; *A. gamb*: *Anopheles gambiae*; *D. mel*: *Drosophila melanogaster*.

(B) Phylogenetic analysis of *CrzR* and *AkhR* based on the alignment of amino acid sequences of insect species. Phylogenetic tree was constructed using MEGA 12 software with the Maximum Likelihood Method and bootstrapped with 10000 replications. The numbers at the nodes of the branches represent the numbers of bootstrap replications supporting that branch.

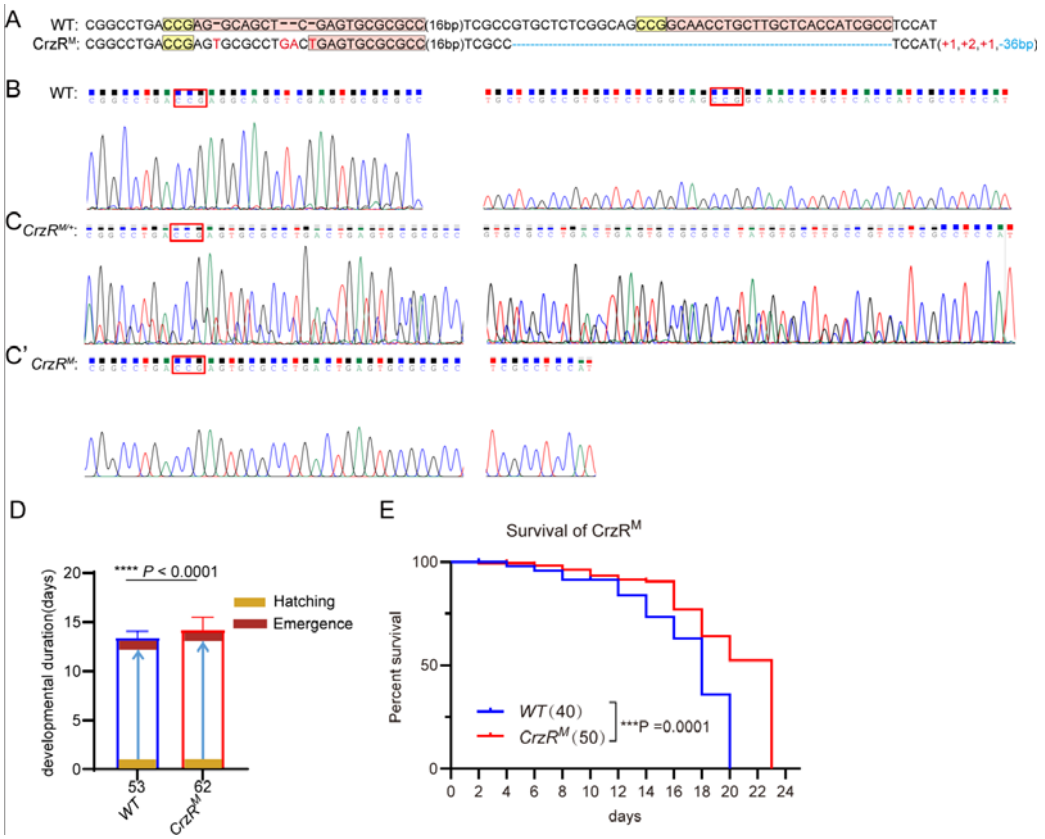

Figure 3 - figure supplement 2. Characterization of *CrzR* mutants in *N. lugens*.

(A) Sanger sequencing of *CrzR* mutants. WT sequence with target (pink), PAM (yellow). Indels: + (insertion), – (deletion).

(B) Sanger sequencing chromatograms of *CrzR* alleles: WT (wild-type).

(C) Sanger sequencing chromatograms of *CrzR* alleles: heterozygous ($CrzR^{M/+}$).

(C') Sanger sequencing chromatograms of *CrzR* alleles: homozygous ($CrzR^{M}$) mutants.

(D) Developmental duration (egg to adult eclosion) in *CrzR* mutants compared to WT. Data: mean ± SD. ****$P < 0.0001$ (Student's *t*-test; n ≥ 40/group).

(E) Survival curves of adult *CrzR* mutants compared to WT. ***$P < 0.001$ (Log-rank Mantel-Cox test; df = 1; n ≥ 50/group).

The *CrzR* is highly expressed in the reproductive organs of female BPHs

To further elucidate the role of the CRZ signaling in regulation of the PMR, we analyzed the *CrzR* expression in *N. lugens* tissues. We first monitored *CrzR* expression by means of RT-PCR and qPCR. Both methods revealed predominant *CrzR* transcript expression in the female reproductive tract (Figure 4A-C). qPCR further demonstrated significantly higher *CrzR* expression in adult females than in males (Figure 4 - figure supplement 1A), particularly localized to female abdomens (Figure 4 - figure supplement 1B).

As we failed to generate a functional NlCrzR antibody, to determine the tissue expression of the receptor in more detail, we used *in situ* hybridization and confirmed strong *CrzR* expression within the female reproductive system (Figure 4D). No hybridization signal was detected in the lateral or common oviducts (Figure 4D1). However, specific labeling occurred in the sperm storage organs: the spermathecae and pouched glands of the lower reproductive tract (Figure 4D2 and 4D2'). These structures are the primary sites for long-term sperm storage. Specificity was validated by absence of signal in sense-probe controls (Figure 4D3 - D4'). This enrichment in sperm storage organs suggests that CRZ signaling may modulate post-mating physiology in part by regulating the mobilization of stored sperm and seminal fluid.

Notably, while CrzR is highly expressed in the female reproductive tract, we acknowledge that RT-PCR and qPCR analyses also detected low but detectable CrzR expression in other tissues, including the CNS and fat body (Figure 4B-C). Thus, we cannot exclude the possibility that *CrzR* in the brain (e.g., by modulating neural

circuits governing reproductive behavior) or fat body (e.g., by affecting post-mating metabolism and nutrient/energy allocation) may also contribute to the PMR. These non-reproductive tract sites of CrzR expression warrant further investigation to fully delineate the systemic roles of CRZ/CrzR signaling in female PMR regulation.

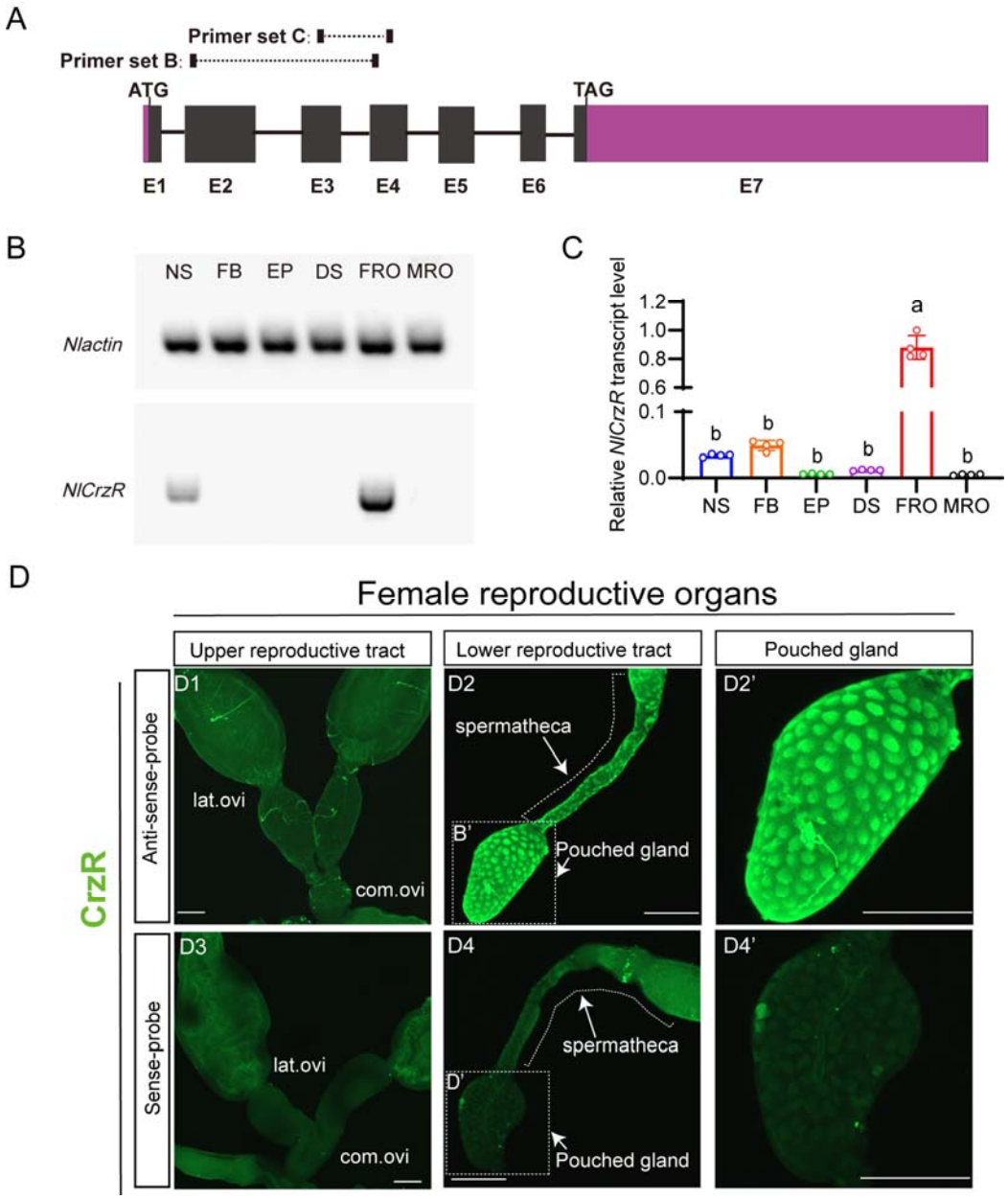

Figure 4. Spatial expression profiling of *CrzR* in the female *N. lugens* reproductive tract.

(A) *CrzR* genomic structure with primer design for experiments in panels B-C.

(B) RT-PCR analysis of *CrzR* tissue distribution. Note weaker expression in central nervous system and fat body. Actin loading control is shown in top row. Tissue abbreviations: NS: central nervous system; FB: fat body; EP: Epidermis; DS: digestive system, FRO: female reproductive organs, MRO: male reproductive organs. Except for the reproductive system, the rest of the tissues come from a mixture of female and male.

(C) qPCR quantification of *CrzR* transcript levels (abbreviations as in B). Data are shown as mean ± s.e.m. Groups that share at least one letter are statistically indistinguishable. One-way ANOVA followed by Tukey's multiple comparisons test.

(D1 - D2') *CrzR* mRNA localization via fluorescent *in situ* hybridization (antisense probe): D1:

There is no signal in lateral/common oviducts; D2/D2': Specific signal is detected in spermatheca (SP) and pouched gland (PG).

(D3 - D4') Negative controls (sense probe) showing background-level signal. Scale bars: 100 µm.

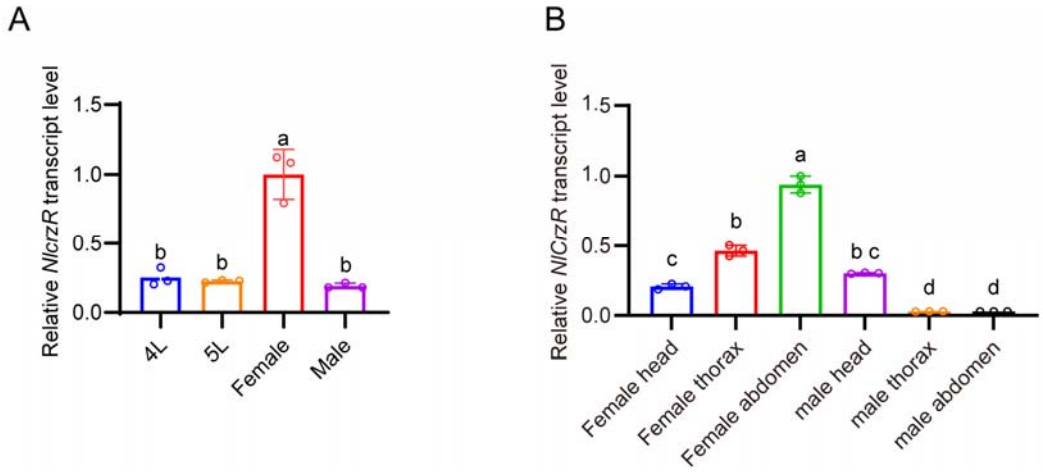

Figure 4 - figure supplement 1. Developmental and tissue-specific expression profiling of *CrzR* in *N. lugens* determined by qPCR.

(A) *CrzR* transcript levels across developmental stages. One-way ANOVA followed by Tukey's multiple comparisons test.

(B) *CrzR* expression in distinct body regions. Data are shown as mean ± SEM shown. One-way ANOVA followed by Tukey's multiple comparisons test.

CRZ signaling in male BPHs impacts the male accessory glands and secondarily modulates the female PMR

Although our primary focus is on CRZ signaling in the female PMR, we also investigated its role in male BPHs, given its established importance in male reproductive biology in *Drosophila* [44,46,48]. In *Drosophila*, silencing CRZ-expressing neurons in the male abdominal ganglia disrupts sperm/seminal fluid transfer and prolongs copulation, while their activation, or CRZ peptide injection, induces rapid ejaculation [44]. To test whether this function is conserved in BPHs, we first injected synthetic CRZ peptide into male BPHs. In contrast to *Drosophila*, CRZ injection did not trigger precocious ejaculation in male BPHs (Figure 5-figure supplement 1A) nor alter the morphology of the male accessory gland (MAG) (Figure 5-figure supplement 1B). However, CRZ-injected males exhibited a significantly reduced mating success rate (defined as the proportion of all tested individuals that successfully court and complete copulation), compared to controls injected with scrambled CRZ (sCRZ) (Figure 5A and B), but maintained unaltered courtship rates (courtship drive) and copulation durations (Figure 5-figure supplement 2A and B).

Since the male mating success rate in some cases was affected by CRZ, we made sure that the female PMR defects do not stem from incomplete male mating: all females included in our PMR analyses were mated with males that had completed full, successful copulation (i.e., completed all mating steps, including seminal fluid transfer, as verified by behavioral observation and subsequent validation of sperm presence in female reproductive tracts). Strikingly, even with fully successful mating, females

mated with CRZ-injected males displayed a severely impaired PMR: nearly 30% of these females re-mated within the test window (vs. 0% of females mated with sCRZ-injected controls) (Figure 5B), and their oviposition was significantly reduced (Figure 5C). Although CRZ injection did not quantitatively change the total protein content of the MAG (Figure 5-figure supplement 1C), we hypothesize that it alters the composition of seminal fluid proteins, consistent with findings in the oriental fruit moth *Grapholita molesta* [49] and thereby reducing the ability to induce a robust female PMR.

In male BPHs, RNAi-mediated knockdown of the *Crz* transcript (via dsNlCrz injection) had no significant effect on key male reproductive behavior: mating success rate (proportion of males that complete copulation), courtship rate (proportion of males exhibiting courtship behaviors such as following or wing display), and copulation duration (Figure 5D and E, Figure 5—figure supplement 2C and D). However, females mated with *dsNlCrz*-injected males exhibited a defective PMR: about 10% remated (Figure 5E) and laid approximately 60% fewer eggs (Figure 5F). Consistent with the RNAi results, males carrying *Crz* mutant alleles (ΔCrz^1 *or* ΔCrz^2) also failed to elicit a full PMR in mated females, despite displaying normal courtship behavior and mating success (Figure 5—figure supplement 2E and F). Specifically, ~25% of the females mated with *Crz* mutant males accepted re-mating (Figure 5G and H), and their egg production was halved compared to females mated with wild-type males (Figure 5I).

Notably, when *Crz* mutant males were crossed with *Crz* mutant females, the PMR defects were dramatically exacerbated: the re-mating rate of females surged to nearly

50%, and egg production plummeted by ~75% relative to wild-type male-female pairs (Figure 5J - L). This near-complete ablation of the PMR underscores that intact CRZ signaling in both sexes is indispensable for triggering a robust PMR in female BPHs.

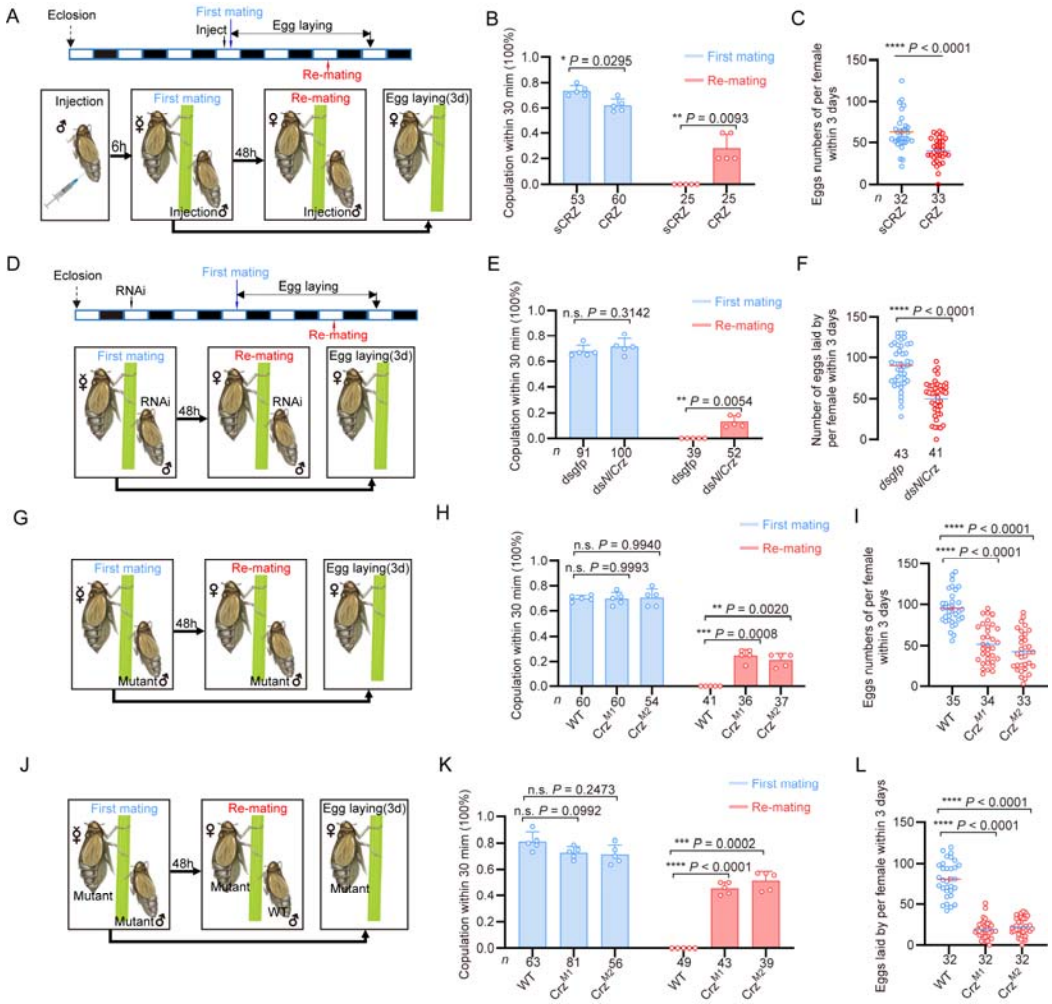

Figure 5. CRZ signaling in male brown planthoppers affects the induction of PMR in females.

(A, D, G, J) Experimental protocols for the behavioral assays presented in panels B/C, E/F, H/I, and K/L, respectively.

(B) Receptivity of virgin and mated wild-type females, scored as the percentage copulating within 30 min when paired with males injected with CRZ (sCRZ as control). Only the re-mating is affected. Small circles indicate the number of replicates; numbers below bars denote total animals. Data are mean ± s.e.m. *P < 0.05, **P < 0.01 (two-way ANOVA followed by Holm-Šídák's multiple comparisons test).

(C) Number of eggs laid per wild-type female within 72 h after mating with males injected with

CRZ (sCRZ as control). Numbers below bars denote total animals. Data are mean ± s.e.m. ***P < 0.001 (Student's t-test). Experiments involved ≥4 biological replicates with ≥ 8 insects per replicate.

(E) Receptivity of virgin and mated wild-type females, scored as the percentage copulating within 30 min when paired with *Crz*-RNAi-treated males (ds*GFP* as control). Again, only re-mating is affected. Small circles indicate the number of replicates; numbers below bars denote total animals. Data are mean ± s.e.m. **P < 0.01, ns (P > 0.05) (two-way ANOVA followed by Holm-Šídák's multiple comparisons test).

(F) Number of eggs laid per wild-type female within 72 h after mating with *Crz*-RNAi-treated males (dsGFP as control). Data are mean ± s.e.m. ****P < 0.0001 (Student's t-test). Experiments involved ≥4 biological replicates with ≥ 8 insects per replicate.

(H) Receptivity of virgin and mated wild-type females, scored as the percentage copulating within 30 min when paired with males of wild type (WT) and CRZ mutants (ΔCrz^{1}, ΔCrz^{2} and $\Delta Crz^{1/2}$). Small circles indicate the number of replicates; numbers below bars denote total animals. Data are mean ± SEM. **P < 0.01, ***P < 0.001, ns (P > 0.05) (two-way ANOVA followed by Holm-Šídák's multiple comparisons test).

(I) Number of eggs laid per wild-type female within 72 h after mating with males of different genotypes (as in H). Numbers below bars denote total animals. Data are mean ± SEM. ****P < 0.0001 (Student's t-test). Experiments involved ≥ 4 biological replicates with ≥ 8 insects per replicate.

(K) Crossing male and female *Crz* mutant insects yield a stronger phenotype than when only males are mutants. Receptivity of virgin and mated females when using *Crz* mutants of both males and females, with wild-type as controls, scored as the percentage copulating within 30 min when paired with males of different genotypes. Compared to Fig. 2H and 2I, double *Crz* knockouts exhibit a stronger effect on receptivity. Small circles indicate the number of replicates; numbers below bars denote total animals. Data are mean ± SEM. ***P < 0.001, ****P < 0.0001, ns (P > 0.05) (two-way ANOVA followed by Holm-Šídák's multiple comparisons test).

(L) Number of eggs laid per female in different genotypic mating combinations. Again phenotypes are stronger compared to those observed with only male mutants (Fig. 2I). Numbers below bars denote total animals. Data are mean ± SEM. ****P < 0.0001 (Student's t-test). Experiments involved ≥4 biological replicates with ≥ 8 insects per replicate.

A

Peptide injection	Ejaculation
Buffer alone	0%(n=30)
sCRZ	0%(n=45)
CRZ	0%(n=50)

Figure 5 - figure supplement 1: The effects of CRZ neuropeptide injection on the behavior and physiology of male BPHs.

(A) CRZ peptide injection into the terminal abdomen of male BPHs does not affect ejaculation. The table shows the ejaculation frequency within 30 minutes post-injection.

(B) Morphology of male BPH accessory glands following *Crz* gene knockout. Representative images show accessory glands from *Crz* mutants and wild-type (WT) controls.

(C) Accessory gland protein content (determined by BCA method assay) after CRZ neuropeptide injection (sCRZ control). Data show mean ± SEM; ns (P > 0.05, Mann–Whitney *U* test).

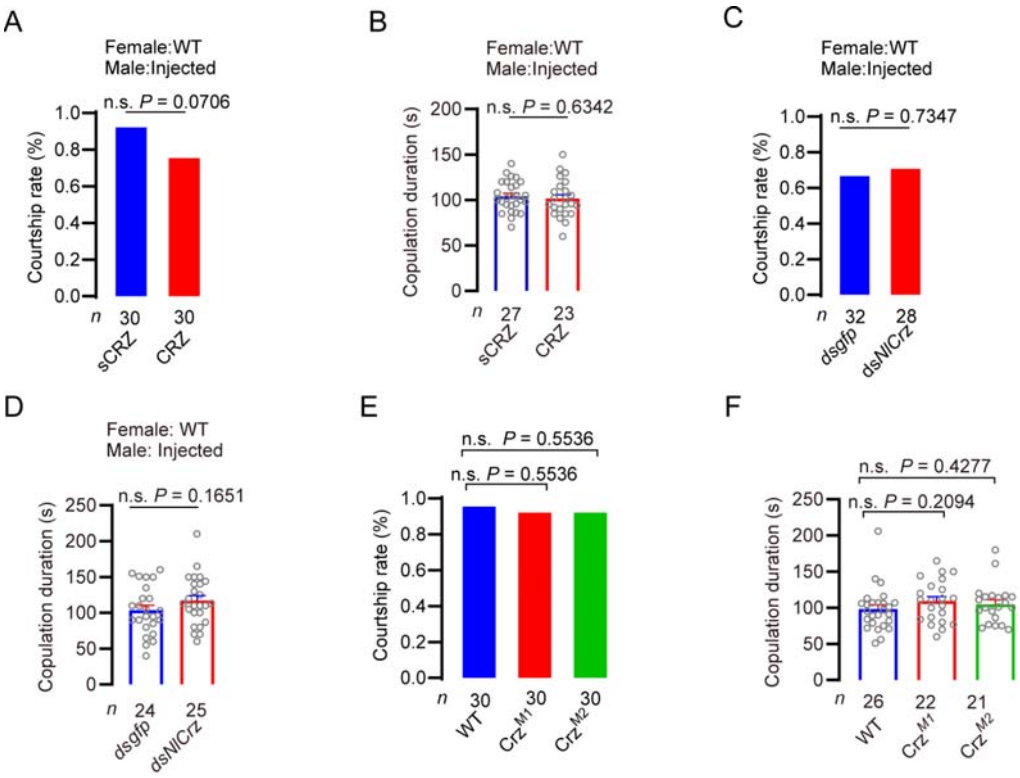

Figure 5 - figure supplement 2. Manipulation of *Crz* in male BPHs does not affect male courtship behavior.

(A) Courtship rate (number of males that exhibit courtship behavior) in males after CRZ peptide injection (sCRZ control) and mating with wild type (WT) females. Numbers below bars

denote total animals. Data represent mean; ns ($P > 0.05$, χ^2 test).

(B) Mating duration of CRZ-injected males paired with WT females (sCRZ control). Data show mean ± SEM; ns ($P > 0.05$, Student's *t*-test).

(C) Courtship rate after *Crz* knockdown via RNAi in males (dsGFP control). Data represent mean; ns ($P > 0.05$, χ^2 test).

(D) Mating duration of *Crz*-knockdown males paired with wild-type females (dsGFP control). Data show mean ± SEM; ns ($P > 0.05$, Student's *t*-test).

(E) Courtship rate of *Crz* mutant males (WT controls). Data represent mean; ns ($P > 0.05$, χ^2 test).

(F) Mating duration of males of different *Crz* mutants paired with WT females. Data show mean ± SEM; ns ($P > 0.05$, Student's *t*-test).

CRZ signaling in male BPHs alters seminal fluid composition

The observation that manipulating *Crz* (via knockdown or mutation) in male BPHs affects the female PMR is particularly intriguing, prompting us to investigate the underlying mechanism. Since we had ruled out production of CRZ in the male reproductive system, including the male accessory gland (MAG), we set out to test whether males with impaired CRZ signaling exhibit defects in basic reproductive performance (e.g., mating success, sperm production/transfer).

To eliminate confounding effects of abnormal sperm production or transfer, we first assessed some key parameters: spermathecal size in females mated to wild-type (WT) or *ΔCrz*^{1} males showed no significant differences (Figure 6A), and sperm counts in the testes of unmated *ΔCrz*^{1} males (vs. WT) and in the spermathecae of females mated to *ΔCrz*^{1} males (vs. WT) were comparable (Figure 6B). These data confirm intact sperm production and transfer, pointing to potential alterations in seminal fluid composition as the driver of female PMR defects. This led us to focus on the protein production in the MAG, encouraged by prior work in the oriental fruit moth (*G. molesta*) where it was shown that CRZ signaling modulates biosynthetic activity in the MAG [49].

To approach this, we performed RNA-sequencing (RNA-seq) on MAGs from WT and *ΔCrz*^{1} males. Comparative transcriptomics identified 2,547 differentially expressed genes (DEGs) in *ΔCrz*^{1} MAGs ($|\log FC| > 1$, FDR < 0.05), with 2,114 upregulated and 431 downregulated (Figure 6C). Notably, 16 genes encoding seminal fluid proteins (SFPs) were dysregulated (7 downregulated, 9 upregulated). Gene Ontology (GO) enrichment analysis of downregulated DEGs revealed significant

overrepresentation of terms related to serine-type endopeptidase activity (GO: 0004252; Padj < 0.05)—a function critical for SFP processing (Figure 6D).

Consistent with transcriptional dysregulation, the total protein content of *ΔCrz*[1] male MAGs was significantly lower than that of WT MAGs, as quantified by the Bicinchoninic Acid (BCA) assay (Figure 6E). Targeted qPCR of specific genes in the MAG confirmed significant downregulation of two genes (Figure 6F and G), and also confirmed unchanged transcript levels of the MAG peptides, *macc* and *ITPL-1,* in mutants (Figure 6H and I). In summary, the transcriptome analysis indicates that CRZ influences the expression of MAG genes and this results in a defective PMR in mated females. Since *macc* and *ITPL-1* are not among the CRZ-regulated genes, some other gene(s) encoding PMR inducing factors need to be identified in future work.

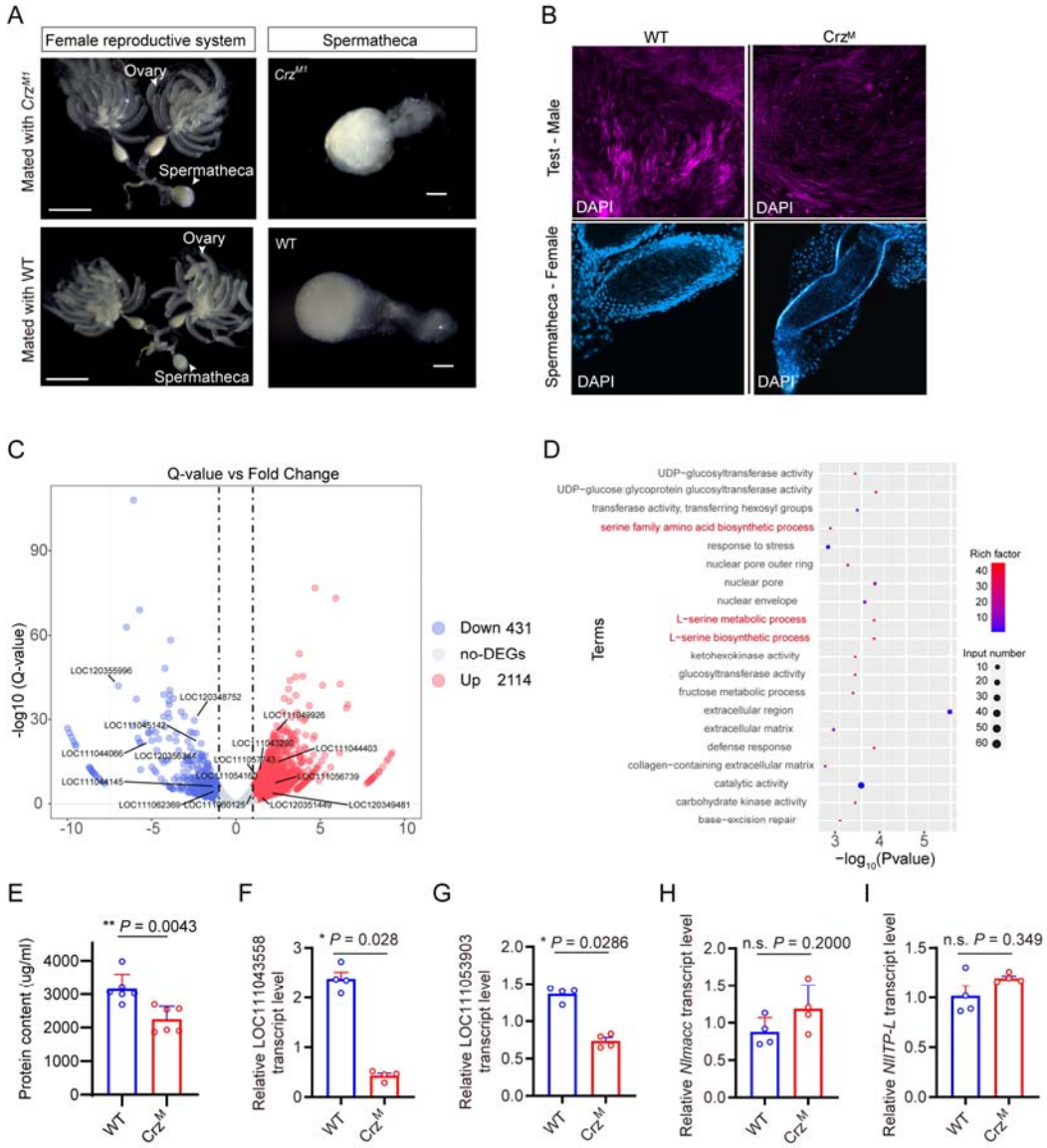

Figure 6. CRZ signaling affects seminal fluid protein composition in male BPHs

(A) Spermathecae of WT females mated to WT or *ΔCrz*[1] males. Scale bar: 1 mm. No morphological differences were observed (n = 15 pairs

(B) DAPI-stained testes (males) and spermathecae (females mated within 4 h) of WT or *ΔCrz*[1] BPHs. Scale bar: 100 μm. Sperm counts showed no genotype-dependent differences (testes: P = 0.32; spermathecae: P = 0.41; n = 12; Mann–Whitney U test).

(C) Volcano plot of differentially expressed genes in male accessory glands (MAGs) from *ΔCrz*[1] mutants versus wild-type (WT) males. Seminal protein genes with significant differential expression ($|\log_2 FC| > 1$, $P < 0.05$) are highlighted (black line). Gene IDs for seminal proteins are annotated. Upregulated genes are shown in red and downregulated in black.

(D) Top 20 enriched Gene Ontology (GO) terms among downregulated genes. Rich factor indicates enrichment strength; input number denotes enriched genes per term.

(E) MAG protein content in WT and *ΔCrz*[1] males measured by BCA method assay. Data: mean

± SEM; ***P* < 0.01 (Mann–Whitney *U* test; *n*= 8 MAG pairs).
(F-I) qPCR validation of seminal fluid genes 43558, 53903, macc and ITP-L in MAGs. Data: mean ± SEM (n = 4 biological replicates). ns: not significant (P > 0.05); *P < 0.05 (Mann–Whitney U test).

Endogenous CRZ signaling modulates aspects of the PMR in female *Drosophila melanogaster*

Having established the critical role of CRZ signaling in regulating the PMR of the female BPH, we next investigated its potential function in female reproduction, including the PMR, of the genetically tractable fly *Drosophila melanogaster*.

We first assessed re-mating frequency in *Crz* mutant female flies (Crz^{attp}). Approximately 40% of the Crz^{attp} females that had experienced a first successful copulation mated again, compared to only 3% of mated wild-type control females (Figure 7A and B). Importantly, the *Crz* mutation did not affect the first mating of females (Figure 7B). Furthermore, mated Crz^{attp} females laid approximately 45% fewer eggs than mated wild-type females (Figure 7C). These results demonstrate that CRZ signaling is necessary for aspects of the PMR in female *Drosophila*, specifically inhibiting re-mating and stimulating post-mating egg production. Immunohistochemical labeling confirmed the absence of CRZ protein in Crz^{attp} mutants (Figure 7D).

To determine whether release of CRZ from *Crz* neurons is responsible for inhibition of remating and stimulation of oviposition, we knocked down *Crz* expression specifically in CRZ-producing neurons using the GAL4-UAS system (*Crz-GAL4* > *UAS-Crz-RNAi*). Consistent with the mutant phenotype, 22% of the mated *Crz-GAL4* >

UAS-Crz-RNAi females mated again after their first successful mating with wild-type males, whereas only 2% of the control females (*Crz-GAL4/+*) did so (Figure 7E). Virgin receptivity was again unaffected by *Crz* knockdown (Figure 7E). Additionally, mated *Crz-GAL4* > *UAS-Crz-RNAi* females laid approximately 20% fewer eggs than mated controls (*Crz-GAL4/+*) (Figure 7F). To further confirm the role of CRZ neuropeptide in modulation of the PMR in females, we injected this peptide in virgin females. Consistent with the above results, CRZ injected virgins displayed a reduced response to mating attempts (Figure 7G). In conclusion, like in BPHs, the neuropeptide CRZ endogenously modulates post-mating behavior also in female *Drosophila*.

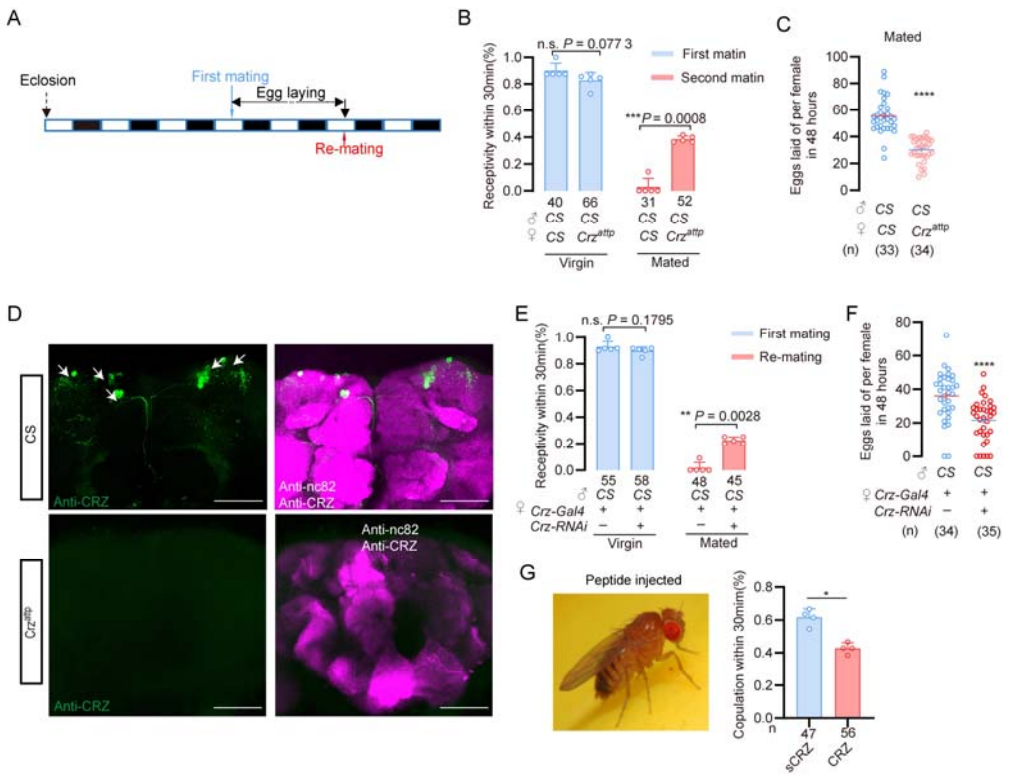

Figure 7. CRZ regulates part of the PMR in *Drosophila melanogaster*.

(A) Schematic of experimental design. White segments on the time axis indicate light periods; black segments indicate dark periods.

(B) Receptivity of virgin and mated *Crz* mutant (*Crz*^{attp}) females, scored as the percentage copulating within 30 min. ***P < 0.001 (Chi-square test).

(C) Mated *Crz* mutants (*Crz*^{attp}) lay more eggs. Graph shows eggs laid per female after mating. ****P < 0.0001 (Student's t-test).

(D) Number of eggs laid per virgin female *Crz* mutants , n.s.: P > 0.05 (Student's t-test).

(E) Anti-CRZ immunostaining in brains of *Crz* mutant (*Crz*^{attp}), control (Cs) and after *Crz* -RNAi). Note CRZ-expressing neurons at arrows in control. Scale bar: 100 µm.

(F) Receptivity of virgin and mated females after *Crz*-RNAi. ****P < 0.0001; Chi quare test.

(G) *Crz*-RNAi reduces the number of eggs laid by mated females. ****P < 0.0001 (Student's *t*-test).

(H) Receptivity of virgin females following CRZ peptide injection (monitored 6 h after injection). *P < 0.05 (Mann-Whitney test).

Discussion

Our study unveils a novel function of CRZ in an endogenous female signaling pathway that modulates the post-mating reproductive behavior and physiology (collectively PMR) in BPHs. It is, thus, the first report linking CRZ to a PMR in insects. In contrast to SP and DUP99B in *Drosophila* [5,18], HP-1 in *Aedes aegypti* [15] and maccessin (macc) recently identified in BPHs [25], CRZ is not produced in the MAG, and thus not transferred from males during copulation. Instead, it is acting as an endogenous peptide derived from neuroendocrine cells in the female brain. Moreover, this CRZ-mediated endogenous modulation in females is seen also in *Drosophila.* When *Crz* is knocked down or knocked out in flies, mated females likewise exhibit an altered PMR.

Interestingly, we found that in BPH males, endogenous CRZ acts on the MAG to affect biosynthesis of seminal fluid proteins (SFP), similar to another insect, the lepidopteran *Grapholita molesta* [49]. That study revealed that silencing the *Crz* gene results in a downregulation of multiple genes in the MAG, including several serine-type endopeptidases, however, the authors did not analyze the effect on the female PMR. Our experiments demonstrate that with impaired CRZ signaling in males the seminal fluid appears to lack some component(s) necessary for inducing a PMR since females mated by *Crz* knockdown males display a reduced PMR. Our gene expression data reveals that neither *macc* nor *ITP-L1* are among the MAG genes affected by *Crz* knockout. These are encoding peptides that are known to induce a partial PMR in female BPHs [25]. Our results therefore suggest that there are additional PMR-inducing factors produced by the MAG of BPHs and that these are regulated by CRZ. Further work is required to identify these factors, but from the present data we can conclude that in BPHs, CRZ signaling influences the female PMR both by action in males and females, but in distinct ways. Similar to our CRZ findings here, a possible dual role of ITPL-1 was also seen in BPHs [25]. This peptide is produced in the MAG, but also in tissues of female BPHs, and knockdown in males results in a reduced PMR in females [25].

Focusing on the endogenous CRZ signaling in female BPHs, our main findings using mutants and RNAi of both *Crz* and *CrzR*, demonstrate that CRZ signaling decreases the female responsiveness to courting males, especially in already mated females. Also, oviposition in mated BPHs is increased by CRZ signaling. CRZ immunolabeling revealed a small set of neurons in the brain and subesophageal ganglion and no CRZ was detected in reproductive organs. Thus, the likely source of CRZ affecting the PMR is the CRZ-producing neuroendocrine cells in the brain. In insects studied so far (including other hemipterans), there are at least three pairs of CRZ expressing lateral neurosecretory cells with axon terminations in the corpora cardiaca [52,53], suggesting that in BPHs and *Drosophila* hormonal CRZ may contribute to the modulation of the PMR. However local CRZ signaling in brain circuits cannot be excluded since the CRZ neurons arborize extensively within the brain.

We found that the CRZ receptor, *CrzR*, is predominantly expressed in the female reproductive tract in BPHs, more specifically in the lower tract including the spermatheca and pouched gland, which are sites of sperm and seminal fluid storage. Thus, in BPHs, CRZ may act to regulate the release of stored sperm and seminal fluid in the female. This regulation would also gate the flow of male-derived factors that induce and maintain the PMR, such as macc and ITPL-1. As mentioned, we cannot exclude additional action of CRZ in neuronal circuits in the CNS that regulate female sexual arousal and reproductive behavior, since our PCR data indicate expression of the *CrzR* also in the CNS. Additionally, the fat body of BPHs, express *CrzR*, similar to *Drosophila* [54], possibly suggesting a role of CRZ in post-mating metabolism.

The brain CRZ neurons of BPHs are likely to be activated by sensory signals from the female reproductive tract upon copulation and hence release CRZ into the circulation (and maybe within the brain). In *Drosophila,* sensory neurons in the reproductive tract are activated by SP (via the SP receptor), and signal via a chain of ascending axons of the VNC to sex-specific neurons in the brain to induce the PMR switch in behavior and physiology [7,35,37,55]. Thus, in *Drosophila,* these sex-specific circuits may also activate the CRZ neurons. Possibly similar sensory and sex-specific neurons exist in BPHs and respond either to mechanical stimuli or factors in the

seminal fluid leading to activation of CRZ neurons and other brain neurons that regulate the PMR.

The female PMR is complex in *Drosophila* and not only receptivity and oviposition are affected, but also feeding, metabolism, sleep patterns and aggression [5,16,18,19,56,57]. In BPHs only the receptivity (and associated rejection behavior) and oviposition have been analyzed in any detail. We found that the MAG-derived peptides transferred with the semen, macc and ITPL-1, only affected the receptivity [25], whereas we show here that CRZ affects also oviposition. Thus, we have identified three different peptides CRZ, macc and ITPL-1 that all influence the PMR in different ways, suggesting complex regulatory mechanisms also in BPHs.

It is interesting to note that CRZ is an evolutionarily conserved neuropeptide that has been found in most, but not all, insect species and it displays a wide array of functions [53,54,58,59]. The CRZ function varies across different insect species, but a common role seems to be in regulation of stress [59-61]. Other functions are for example: in the American cockroach, CRZ accelerates the heart rate [62], in locusts, it triggers the formation of pigments that darken the body color in gregarious insects [63], in the moth *Bombyx mori*, CRZ affects developmental speed and reduces the rate of silk spinning behavior [64]; in *Drosophila* larvae, CRZ regulates molting motor behavior [65] and growth [66]; in adult *Drosophila* CRZ regulates stress responses, food intake and metabolism [54,67], and protein food preference [12], as well as sperm ejection and mating duration in males [42]; and in social ants, it regulates the social hierarchy and inhibits egg-laying in the queen [45]. Finally, a recent study found that CRZ mediates a diapause-induced suppression of reproduction in female bean bugs [68]. To all these functions can now be added the role of CRZ in reproductive behavior and physiology of BPHs, especially in the female PMR of BPHs and *Drosophila*. However, we also found a role of CRZ signaling in regulating the production of seminal fluid proteins in the MAG. Finally, building on the role of CRZ in metabolism in *Drosophila* [54], it is possible that CRZ also regulates post-mating metabolism in female BPHs. Thus, there may be a link between CRZ and the altered feeding and metabolism commonly seen in mated female insects.

806

807 **Table 1. Primers used in this study**

Primer name	Sequence (5'-3')	Purpose
NlCrz-F	ACCGCATCAGGACGACAATA	Gene clone
NlCrz-R	ACCATAGCTGTTGAGCTACAAAT	
NlCrz-RNAi-F	TAATACGACTCACTATAGGGGCTAGTGTTGCAATGCTGTTG	*dsNlCrz* synthesis
NlCrz-RNAi-R	TAATACGACTCACTATAGGGGCTGTTGAGCGTTAGACTGT	
QNlCrz-F	AGACAGTGACCACAGCTCAA	qRT-PCR for NlCrz
QNlCrz-R	GAGTACTGGAACGTCTGTGC	
NlCrz-sgRNA-F1	TAATACGACTCACTATAGGCACAGGAGTGATGCAGAC	sgRNA synthesis for NlCrz knock-out
NlCrz-sgRNA-R1	TTCTAGCTCTAAAACGTCTGCATCACTCCTGTGCC	
NlCrz-sgRNA-F2	TAATACGACTCACTATAGCTACTAGTGCTGGGCTGCA	sgRNA synthesis for NlCrz knock-out
NlCrz-sgRNA-R2	TTCTAGCTCTAAAACTGCAGCCCAGCACTAGTAGC	
NlCrz Check F	ACCATAGCTGTTGAGCTACAAAT	To analyze NlCrz mutant
NlCrz Check R	TGCAATGCTGTTGTCGCGAC	
NlCrzR-F	AATCAGGCGATGAACCTCAGTT	Gene clone
NlCrzR-R	ACGCAGTTCTATGACGTGAGG	
NlCrzR-RNAi-F	TAATACGACTCACTATAGGGCGCCGTCTACACACTCATCT	*dsNlCrzR* synthesis
NlCrzR-RNAi-R	TAATACGACTCACTATAGGGCTACCAGCTTCGTACAGCGT	
QNlCrzR-F1	CTGGTGCTAATAGGGCTGGA	qRT-PCR for NlCrzR
QNlCrzR-R1	TCCGGTGTACAGTTGCTCTT	
QNlCrzR-F2	TGCTCACCATCGCCTCTATC	qRT-PCR for NlCrzR
QNlCrzR-R2	TGCCATGGTTCCGTGTAGAA	
NlCrzR-F1	CCCACTAGCCAGCAACCATT	RT-PCR for NlCrzR
NlCrzR-R1	TCCTCCACAAATGGTCCACG	
NlCrzR-sgRNA-F1	TAATACGACTCACTATAGGCACGCACTCGAGCTGCCT	sgRNA synthesis for NlCrzR knock-out
NlCrzR-sgRNA-R1	TTCTAGCTCTAAAACAGGCAGCTCGAGTGCGTGCC	
NlCrzR-sgRNA-F2	TAATACGACTCACTATAGGCGATGGTGAGCAGGTTGC	sgRNA synthesis for NlCrzR knock-out
NlCrzR-sgRNA-R2	TTCTAGCTCTAAAACGCAACCTGCTCACCATCGCC	
NlCrzR Check-F	GGCAGCAACCTGAGCCACCC	To analyze NlCrzR mutant
NlCrzR Check-R	GTCTTACCAGCGACCCAAGC	

QNlvg-F	GTGGCTCGTTCAAGGTTATGG	qRT-PCR for Nlvitellogenin
QNlvg-R	GCAATCTCTGGGTGCTGTTG	
QNlvgR-F	AGGCAGCCACACAGATAACCGC	qRT-PCR for Nlvitellogenin receptor
QNlvgR-R	AGCCGCTCGCTCCAGAACATT	
QNl53903-R	GTCCACCGAACTTTTCCTGG	
QNl Macc-F	TCTTTGGAAGTGGTGATTCCATCT	qRT-PCR for NlMacc
QNl macc-R	TGTCTACTTCACATACATGTGGCT	
QNl itpl-1-F	GATCAGATTCAATTCACATTCCTC	qRT-PCR for Nlitpl-1
QNl itpl-1-R	AGATTGTAGCAGTCCTCGCATA	

Key resources table

REAGENT or RESOURCE	Source or reference	Identifiers
Antibodies		
Goat anti-Rabbit Alexa 488	Invitrogen	Cat#A11008; RRID: AB_143165
Goat anti-mouse Alexa 488	Invitrogen	Cat#A28175; RRID: AB_2536161
Goat anti-mouse Alexa 555	Invitrogen	Cat# A21428; RRID: AB_2535849
Anti-CRZ	Gift from Prof. Jan A. Veenstra	
Chemicals, Peptides, and Recombinant Proteins		
4% PFA	Leagene	Cat# DF0134
DAPI	Solarbio	Cat# C0060
PBS	Solarbio	Cat# P1022
ReadyProbes 2.5% Normal Goat Serum	Invitrogen	Cat# R37624
Experimental Models: Organisms/Strains		
Canton-S	Bloomington Drosophila Stock Center	64349
Crz^{attp}	Rao and Deng et al., 2019	BDSC: 84487
Crz-GAL4	Bloomington Drosophila Stock Center	51976
Crz-RNAi	Tsinghua Fly Center	THU2139
Software and Algorithms		
FIJI		https://doi.org/10.1038/nmeth.2019
Prism 9	GraphPad	RRID: SCR_002798
Photoshop	Adobe	RRID: SCR_014199
Illustrator	Adobe	RRID: SCR_010279
ZEN	Zeiss	N/A
Motic Images Plus3.0	Motic	N/A
Motic Images Devices	Motic	N/A
Other		
Egg-laying device	Gou et al., 2016	N/A
Anatomical tweezers	Dumont	Cat# 0209-5-PO

Method details

Experiment insects

All the brown planthoppers used in this research were collected from Hangzhou, Zhejiang Province in 1995. The insects were kept indoors on fresh rice seedlings (Taichung Native 1, TN1) in a growth chamber at 27 ± 1 °C and 70 ± 10% relative humidity, under a 16 h:8 h (Light: Dark) photoperiod [69].

All *Drosophila* stocks were raised in standard cornmeal–molasses–agar medium maintained at 25° C, 60% humidity, and under 12 hr:12 hr light:dark conditions. We used Canton s flies as the wild-type strain. The relevant information of fruit flies used in the experiments are shown in key resources table.

Behavior assays of *Nilaparvata lugens*

Mating and receptivity

All BPHs were raised in incubators with a 16 h:8 h dark:light cycle. Unmated female and male BPHs were collected within 12 hours of emergence. For RNAi or neuropeptide injection treatment, the protocol is shown in Figure 1A and Figure 1D. The mating behavior (or female receptivity behavior) test in this study usually conducted the first mating between 3 and 5 days after emergence. The mating experiment was completed in a plastic tube (2.5cm in diameter and 10cm in height). Fresh rice seedlings of appropriate length were placed in each tube, and then a female and male BPHs were added. The mating conditions and other reproductive behavior parameters during this period were observed in a constant temperature room at 25℃ for 30min, and the males were taken out after 30 min. For the experiment requiring a second mating, females successfully mated for the first time were retained. After 48 hours, wild-type males were put in for the re-mating test. The males in all secondary mating experiments were wild type. The monitoring time for each mating behavior was 30 minutes; the receptivity rate refers to the proportion of successful matings of female individuals within the 30-minute measurement period.

Egg laying

After completing the first mating, the male is sucked out and a sufficient number of rice seedlings are added to the tube, and the female is retained to lay eggs in the tube. After 72 hours, the spawning female is transferred out of the tube. After the eggs have matured, about 4-5 days later, we used tweezers to gently manipulate the rice seedlings and counted the number of fertilized eggs produced by the females. Note that 4 to 5 days after the egg is produced, the successfully fertilized egg will display red eye-spots. (Oviposition assay protocol: For quantitative assessment of post-mating responses, egg-laying activity was monitored over a 72-hour observation window following verified initial copulation. To eliminate confounding effects from sequential mating trials, experimental subjects undergoing oviposition measurement were permanently excluded from subsequent re-mating evaluations.)

To determine the oviposition profile of females injected with CRZ peptide. virgin female or mated female BPHs that had emerged 3-5 days earlier were transferred into plastic tubes with sufficient amount of rice seedlings 6h after recovery from CRZ injection, and the BPHs were taken out 24 hours later，using tweezers to gently dissect the rice seedlings the number of fertilized eggs produced by the females were counted.

Courtship rate

During the mating assessment, an unmated (virgin) female and an unmated male BPH was placed in a plastic tube containing rice seedlings. The occurence of courtship behavior in the male individuals was recorded, which included a series of courtship actions such as following, wing display, licking, and attempting to mate. The proportion of individuals displaying courtship behavior among all experimental individuals is defined as the courtship rate.

Copulation duration

During the mating assessment, an unmated (virgin) female and an unmated male BPH were placed in a plastic tube containing rice seedlings. Timing begins when mating

behavior is observed between the female and male, and stops immediately after completed copulation. The duration from the start of the mating behavior to its conclusion is defined as the mating duration.

Behavior assays of *Drosophila melanogaster*

Mating and re-mating：During the receptivity assessment, all experimental fruit flies were virgin flies that emerged within 12 hours in a 20°C incubator in a 12 h:12 h dark:light cycle. After collection, they were kept at 25°C incubator in a 12 h:12 h dark:light cycle for 4 days before behavioral testing. Receptivity behavior measurement：a perforated plate was placed on top of a non-perforated plate. Male fruit flies were briefly anesthetized on ice and gently transferred into the holes of the perforated plate, with one male per hole. Once the male transfer was completed, a plastic film was gently placed over the perforated plate, followed by covering it with another perforated plate. Then, the virgin female fruit fly, also anesthetized on ice, was placed in each hole. After the transfer was completed, a non-perforated plate was placed on top. This setup was then transferred to a 25°C incubator to acclimate for 30 minutes. The plastic film separating the male and female flies was quickly removed, and video recording began for 30 minutes. The recorded videos were analyzed to calculate the acceptance rate of the females. Successful mating females were collected and individually transferred into plastic tubes containing sufficient artificial food for fruit flies to lay eggs. After 24 hours of laying eggs, the female flies were transferred to a new finger-shaped tube with ample artificial feed for another 24 hours of laying. After 48 hours, these egg-laying females were subjected to a secondary mating assessment with wild-type, unmated males, using the same method as described above, to evaluate the acceptance rate during the second mating process. Additionally, the number of eggs laid by each female during the 48 hours was recorded.

Egg laying for mated females：First, collect virgin female fruit flies that eclosion within 12 hours at 20°C incubator in a 12 h:12 h dark:light cycle and then keep them in a 25°C incubator in a 12 h:12 h dark:light cycle for 4 days. After that, unmated males of the wild type and virgin females were mixed 1:1.5 times. 24 hours after full mating, female flies

were lightly anesthetized with ice and transferred to plastic vials containing enough artificial fruit fly food for them to lay eggs for 24 hours. After 24 hours, the flies were transferred again to a new bottle full of artificial food for another 24 hours of egg laying. The number of eggs in each vial is calculated under a microscope, and the total number of eggs in the two vials of each female fruit fly represents the egg-laying capacity of that individual.

Developmental duration statistics

Nymphs of BPHs that hatched synchronously from distinct genotypes were collected and reared in plastic cups containing fresh rice seedlings; the seedlings were replaced regularly to maintain optimal conditions. From the day the nymphs reached the fifth instar, cups were inspected daily for adult emergence, and the number of newly emerged adults was recorded. After all surviving individuals had completed eclosion, the total nymph-to-adult developmental duration was calculated.

BPHs survival rate statistics

For neuropeptide injection: After 4-day emergence, virgin BPHs were injected with CRZ neuropeptide or scrambled CRZ, and after 6 hours of recovery, these insects were placed into a plastic tube with sufficient quantity of rice seedlings. Survival was monitored every 24 hours until all specimens were dead.

For mutant: Wild-type and mutant BPHs adults that eclosed on the same day were individually confined in plastic tubes, each supplied with ample fresh rice seedlings and water renewed regularly to ensure optimal living and nutritional conditions. The number of surviving individuals of each genotype was recorded every 24 h until all had died, and survival curves were generated from these data.

Neuropeptide synthesis and injection.

Corazonin (CRZ) and scrambled CRZ (sCRZ) were synthesized by Genscript Co. Ltd (Nanjing, China). Peptide masses were confirmed by Mass spectrometry and the amount of peptide was quantified by amino acid analysis. The amino acid sequences of the

peptides used in this study are: *N. lugens* corazonin: pQTFQYSRGWNamide; scrambled corazonin: pQSRYTTFGQWTNamide. On the fourth day after adult emergence, virgin female BPHs were injected with different concentrations of synthetic CRZ peptide and control scrambled peptide. The scrambled peptide control was used to monitor for potential non-specific effects on behavior due to the process of injection. Each mg peptide was dissolved in 100 μl DMSO solution (Acmec, #D54264), and then diluted to 1.5 mM, 0.15 mM, 0.015 mM and 0.0015 mM with 1×PBS as solvent. The BPHs were anesthetized with CO_2 for about 30 seconds and placed abdomen up on 2% agarose (Solarbia, #A8201) plate and 50 nl neuropeptide solution injected into each female, 30 nl neuropeptide solution injected into each male. The male virgins were injected on the third day of emergence. Six hours after neuropeptide injection the insects were used for behavior assay.

Protein concentration determination of male accessory glands

MAGs of 3-day-old unmated males (n = 48) were dissected in 1×PBS(Solarbio, #P1020) and then gently crushed in 60 μL of 1×PBS. The tissues were homogenized for 60 s and centrifuged at 10,000g for 15 min at 4° C and the supernatant removed. The protein concentration in the supernatant was determined using the BCA Protein Assay Kit (CWBIO, #CW0014S).

Gene cloning and sequence analysis

We used the NCBI database with BLAST programs to carry out sequence alignment and analysis. Then we predicted Open Reading Frames (ORFs) with EditSeq. The primers were designed by Primer designing tool in NCBI. Total RNA Extraction was using the TRIzol reagent (Invitrogen, Carlsbad, CA, USA) according to the manufacturer's instructions. The cDNA template used for cloning was synthesized using the Biotech M-MLV reverse transcription kit and the synthesized cDNA template was stored at -20˚C. The transmembrane segments and topology of proteins were predicted by TMHMM v2.0 (http://www.cbs.dtu.dk/services/TMHMM-2.0/) [70]. Multiple alignments of the complete

amino acid sequences were performed with Clustal Omega (http://www.ebi.ac.uk/Tools/msa/clustalo).

qRT-PCR for spatial expression pattern and RNAi efficiency

The nervous system (NS), fat body (Fb), digestive system (DS), epidermis (EP), male reproductive organs (MRO) and female reproductive organs (FRO) from 3-5 days old adults were dissected in 1×PBS, to determine the tissue-specific expression pattern. With the exception of the reproductive system, the rest of the tissue comes from both sexes equally. The adult BPHs were placed on ice under slight anesthesia and dissected under a stereoscopic microscope (ZEISS). At least 50 individuals were dissected as one sample for tissue-specific analysis with three replicates. All tissues were quickly transferred to Trizol (Invitrogen, Carlsbad, CA, USA) solution at 0° C after dissection.

For RNAi efficiency testing, we collected the whole bodies of BPHs and transferred to a 1.5 mL EP tube containing Trizol reagent. Total RNA extraction was using Trizol reagent (Invitrogen, Carlsbad, CA, USA) according to the manufacturer's instructions. The cDNA template used for cloning was synthesized using the Biotech M-MLV reverse transcription kit and the synthesized cDNA template was stored at -20˚C.

Real-time qPCRs of the various samples used the UltraSYBR Mixture (with ROX) Kit (CWBIO, Beijing, China). The PCR was performed in 20μl reaction including 2 μl of 10-fold diluted cDNA, 1 μl of each primer (10 μM), 10μl 2 × UltraSYBR Mixture, and 6 μl RNase-free water. The PCR conditions used were as follows: initial incubation at 95˚C for 10 min, followed by 40 cycles of 95˚C for 10 s and 60˚C for 45 s. *N. lugens* 18S rRNA and actin were used as an internal control (primers listed in Table1). Relative quantification was performed via the comparative $2^{-\Delta\Delta CT}$ method [71].

RNAi and RNAi efficiency determination

For lab-synthesized dsRNA, *gfp*, Nl*CrzR* and Nl*Crz* were amplified by PCR using specific primers conjugated with the T7 RNA polymerase promoter (primers listed in Table1). dsRNA was synthesized by the MEGAscript T7 transcription kit (Ambion, Austin, TX, USA) according to the manufacturer's instructions. Finally, the quality and size of the dsRNA

989 products were verified by 1% agarose gel electrophoresis and the Nanodrop 1000
990 spectrophotometer and kept at -70˚C until use.
991 3-5 days old virgin female and virgin male BPHs were used for injection of 50nl / 30nl of 5
992 μg/μl dsRNA per insect. Injection of an equal volume of ds*gfp* was used as negative
993 control. After 48 hours, the insects were used behavior assays and gene relative
994 expression analysis.
995
996 **Neuropeptide injection after RNAi**
997 48 hours after the ds*CrzR* injection, each insect was injected again with 10 ng of peptide
998 dissolved in 50 nL of 1 × PBS balanced salt solution. Recovery was for six hours after
999 injection. These insects were used for behavior assays. RNAi efficiency was examined by
1000 qPCR using a pool of ten individuals 48 hours after dsRNA injections.
1001
1002 **In vitro synthesis of sgRNA and Cas9 mRNA**
1003 The single guide RNA (sgRNA) was designed as previously reported [72]. Briefly, sgRNA
1004 was designed by manually searching genomic sequence around the region of the *Crz* and
1005 *CrzR* exon for the sequences corresponding to 5'-$N_{17\text{-}20}$NGG-3', where NGG is the
1006 protospacer-adjacent motif (PAM) of SpCas9 and N is any nucleotide. For in vitro
1007 transcription of sgRNA, were synthesized in vitro using the GeneArt™Precision gRNA
1008 Synthesis Kit (Thermo Fisher Scientific, Vilnius, Lithuania) according to the instructions of
1009 manufacturer. The Cas9 protein (TrueCut™Cas9 Protein v2, Cat. NO. A36497) was
1010 purchased from Thermo Fisher Scientific (Shanghai, China).
1011
1012 **Embryo microinjection, crossing and genotyping**
1013 The embryonic injection was performed as previously reported [73]. The female BPHs,
1014 which had been mated for 3-6 days after emergence, were selected to lay eggs on fresh
1015 rice leaves. After 30 minutes, the embryos were transferred onto double-sided tape
1016 attached to a microscope slide along the long edge by gently pressing the slide onto the
1017 dorsal surface of embryos. A few drops of halocarbon oil 700 was added to these eggs.
1018 About 0.5–1 nL mixture of Cas9 protein (200 ng/μL) and sgRNA (100 ng/μL) was injected

into each egg using a FemtoJet and Inject Man NI 2 microinjection system (Eppendorf, Germany). After the injection, the eggs were placed in Petri dishes covered with moist filter paper, and the Petri dishes were placed in plant growth chamber at 27±1 °C, 70±10% RH for hatching. These eggs hatched into G0 generations.

Crossing and genotyping (Re-edit)

To establish homozygous mutants of Nilaparvata lugens through CRISPR-mediated gene editing, newly emerged G0 adults were outcrossed with wild-type counterparts to generate G1 progeny. Following successful mating and oviposition, genomic DNA was extracted from G0 adults for mutation screening. The target region surrounding NlCrzR was amplified by PCR using specific primers NlCrzR-check-F and NlCrzR-check-R (primer sequences listed in Table 1), followed by Sanger sequencing to identify G0 individuals carrying mutations.

Progeny (G1) from mutation-positive G0 parents were maintained through sibling crosses to establish G2 populations. Subsequent genotyping via Sanger sequencing was performed on G1 individuals to select breeding pairs where both male and female parents carried heterozygous mutations. The resulting G2 offspring from these validated pairs were then subjected to intercrossing to ultimately generate homozygous mutant lines.

Quantitative RT-PCR

The first-strand cDNA was synthesized with HiScript II Q RT SuperMix for qPCR (+gDNA wiper) kit (Vazyme, Nanjing, China) using an oligo (dT)18 primer and 500 ng total RNA template in a 10 μl reaction, following the instructions. Real-time qPCRs in the various samples used the UltraSYBR Mixture (with ROX) Kit (CWBIO, Beijing, China). The PCR was performed in 20 μl reaction including 4 μl of 10-fold diluted cDNA, 1 μl of each primer (10 μM), 10 μl 2 × UltraSYBR Mixture, and 6 μl RNase-free water. The PCR conditions used were as follows: initial incubation at 95˚C for 10 min, followed by 40 cycles of 95˚C for 10 s and 60˚C for 45 s. *N. lugens* 18S rRNA or *Drosophila* rp49 were used as an internal control (Table 1). Relative quantification was performed via the comparative $2^{-\Delta\Delta CT}$ method (Livak, K. J,2001).

Immunohistochemistry

Adult BPHs, 3-5 days old, were dissected under 1x phosphate-buffered saline (PBS; pH 7.4) in Schneider's insect medium (S2). We dissected the brain, ventral nerve cord and reproductive system of the BPHs. These tissues were fixed in 4% paraformaldehyde in PBS for 30 min at room temperature. After extensive washing with PTX (0.5% Triton X100, 0.5% bovine serum albumin in PBS), blocked in 3% normal goat serum. Then, the tissues were incubated in Anti - CRZ for 12 hours at 4℃ and in secondary antibody for 12 h at 4℃. Primary antibodies used were: rabbit anti - CRZ (1:1000, Anti - CRZ was gift from Jan A. Veenstra), mouse anti-Bruchpilot (1:1000, Developmental Studies Hybridoma Bank nc82). Secondary antibodies used: donkey anti-rabbit IgG conjugated to Alexa 488 (1:500, R37118, Thermo Fisher Scientific) and donkey anti-mouse IgG conjugated to Alexa Alexa 555 (1:500, R37115, Thermo Fisher Scientific). The samples were mounted in Vectorshield (Vector Laboratory). Images were acquired with Zeiss LSM 700 confocal microscopes, and were processed with Image J software. All antibodies were diluted in PTX solution. The primary antibody was diluted at a ratio of 1:1000, while the secondary antibody was diluted at a ratio of 1:500.

Adult female *Drosophila melanogaster*, 3-5 days old, were dissected under 1 x phosphate-buffered saline (PBS; pH 7.4) in Schneider's insect medium (S2). We dissected the brain, ventral nerve cord and reproductive system. These tissues were fixed in 4% paraformaldehyde in PBS for 30 min at room temperature. After extensive washing with PTX (0.5% Triton X100, 0.5% bovine serum albumin in PBS), blocked in 3% normal goat serum. Then, the tissues were incubated in Anti - CRZ and Anti - nc82 for 12 hours at 4℃ and in secondary antibody for 12 h at 4℃. Primary antibodies used were: rabbit anti-CRZ (1:1000, A11122, Provided by Jan A. Veenstra). Secondary antibodies used: donkey anti-rabbit IgG conjugated to Alexa 488 and anti-mouse IgG conjugated to Alexa 555 (R37118, Thermo Fisher Scientific). The samples were mounted in Vectorshield (Vector Laboratory). Images were acquired with Zeiss LSM 700 confocal microscopes, and were processed with Image J software. All antibodies were diluted in PTX solution.

Fluorscent in situ hybridization (FISH)

FISH was performed as previously reported by Yan et al. [74]. Briefly, the reproductive system of the female BPH dissection was performed under 1x Phosphate Buffered Saline (PBS) supplemented with a protease and phosphatase inhibitor cocktail (Shyuanye, #R40012) on a clean, clear rubber pad using two fine forceps (Dumont, #0108-5-po). Dissected tissues were fixed using 4% paraformaldehyde (PFA) (Shyuanye, #22039) diluted in 1 x PBS with 0.1% Tween20 (0.1% PBST) at room temperature (RT) for 20 min on a shaker. Fixed tissues were washed three times with 0.1% PBST for 15 min each on a shaker. The tissues were dehydrated in 25%, 50%, 90% and 100% methanol, and then rehydrated in reverse order, performed at room temperature for 10 minutes at a time. The tissue was then washed twice with 0.1% PBST and shaken for 5 minutes. A post fixation was performed by incubating the tissue in 4% PFA in 1 x PBS on a shaker for 20 minutes, followed by two washes with PBST for 5 minutes each while shaking. The tissue was permeabilized with proteinase K (10 µg/ml) at room temperature for 2 minutes. After incubation, the tissue was washed with 0.1% PBST for 5 minutes while shaking. The PBST was removed, and pre-hybridization solution (Boster, #AR0152) was applied at 55°C for approximately 2 hours. The DIG probes were denatured in a metal bath at 80°C for 5 minutes and then immediately placed on ice. The denatured DIG-labeled probes were added to the hybridization solution, and hybridization was carried out overnight at 55°C. Then, the hybridized tissue was washed twice at 55°C for 40 minutes with warm pre-hybridization solution, followed by four washes at room temperature with 0.1% PBST for 10 minutes each. The detection of the DIG-labeled probes was performed using an anti-DIG conjugated fluorescent antibody (1:100 dilution, Jackson, #200-542-156), incubated at room temperature in 0.1% PBST for 2 hours, followed by three washes with 0.1% PBST. Finally, the tissue was mounted in mounting medium and imaged using a Zeiss confocal microscope.

Imaging of reproductive organs

Male BPHs of different genotypes and different treatments, and female BPHs mated

with males of different genotypes, were used for dissecting reproductive organs on the fourth day after emergence. Motic Images Devices and Motic Images Plus 3.0 were used to capture images of these reproductive organs.

Quantification and statistical analysis

All graphs were generated using Prism 9 software (GraphPad Software, La Jolla, CA). Data presented in this study were first verified for normal distribution by D'Agostino– Pearson normality test. If normally distributed, Student's *t* test was used for pairwise comparisons, and one-way ANOVA or two-way ANOVA was used for comparisons among multiple groups. If not normally distributed, Mann–Whitney test was used for pairwise comparisons, and Kruskal–Wallis test was used for comparisons among multiple groups, followed by Dunn's multiple comparisons. All data are presented as mean ± s.e.m.

Data availability statement: All of the RNA sequence data in this article have been deposited in the China National Center for Bioinformation database and are accessible in PRJCA045433.

ACKNOWLEDGMENTS: We thank Dr. Jan A. Veenstra for providing CRZ antibody. This project was supported by National Key R&D Program of China (2022YFD1700200) to S.-F.W., the National Natural Science Foundation of China (No. 32022011 & 32472542) to S.-F.W..

References:

1. Do-Hyoung Kima , Y.-Hoon J., , Minsik Y., and , K.-Min L., and Young-Joon Kima,1 (2024). Long-term neuropeptide modulation of female sexual drive via the TRP channel in Drosophila melanogaster. Proceedings of the National Academy of Sciences. 10.1073/pnas.
2. Sun, M., Ma, M., Deng, B., Li, N., Peng, Q., and Pan, Y. (2023). A neural pathway underlying hunger modulation of sexual receptivity in Drosophila females. Cell Rep *42*. 10.1016/j.celrep.2023.113243.
3. Wang, F., Wang, K., Forknall, N., Parekh, R., and Dickson, B.J. (2020). Circuit and Behavioral Mechanisms of Sexual Rejection by Drosophila Females. Current biology : CB. 10.1016/j.cub.2020.07.083.
4. Wang, K., Wang, F., Forknall, N., Yang, T., Patrick, C., Parekh, R., and Dickson, B.J. (2021). Neural circuit mechanisms of sexual receptivity in Drosophila females. Nature *589*, 577-581. 10.1038/s41586-020-2972-7.
5. Kubli, E. (2003). Sex-peptides: seminal peptides of the Drosophila male. Cell Mol Life Sci *60*, 1689-1704. 10.1007/s00018-003-3052.
6. Yapici, N., Kim, Y.J., Ribeiro, C., and Dickson, B.J. (2008). A receptor that mediates the post-mating switch in Drosophila reproductive behaviour. Nature *451*, 33-37. 10.1038/nature06483.
7. Yang, C.H., Rumpf, S., Xiang, Y., Gordon, M.D., Song, W., Jan, L.Y., and Jan, Y.N. (2009). Control of the postmating behavioral switch in Drosophila females by internal sensory neurons. Neuron *61*, 519-526. 10.1016/j.neuron.2008.12.021.
8. Rezaval, C., Pavlou, H.J., Dornan, A.J., Chan, Y.B., Kravitz, E.A., and Goodwin, S.F. (2012). Neural circuitry underlying Drosophila female postmating behavioral responses. Current biology : CB *22*, 1155-1165. 10.1016/j.cub.2012.04.062.
9. Camus, M.F., Huang, C.C., Reuter, M., and Fowler, K. (2018). Dietary choices are influenced by genotype, mating status, and sex in Drosophila melanogaster. Ecol Evol *8*, 5385-5393. 10.1002/ece3.4055.
10. Craig, G.B., Jr. (1967). Mosquitoes: female monogamy induced by male accessory gland substance. Science *156*, 1499-1501. 10.1126/science.156.3781.1499.
11. Judson, C.L. (1967). Feeding and oviposition behavior in the mosquito Aedes aegypti (L.). I. Preliminary studies of physiological control mechanisms. Biol Bull *133*, 369-378. 10.2307/1539832.
12. Liu, C., Tian, N., Chang, P., and Zhang, W. (2024). Mating reconciles fitness and fecundity by switching diet preference in flies. Nature communications *15*, 9912. 10.1038/s41467-024-54369-w.
13. Liu, H., and Kubli, E. (2003). Sex-peptide is the molecular basis of the sperm effect in Drosophila melanogaster. Proceedings of the National Academy of Sciences of the United States of America *100*, 9929-9933. 10.1073/pnas.1631700100.
14. Chapman, T., Bangham, J., Vinti, G., Seifried, B., Lung, O., Wolfner, M.F., Smith, H.K., and Partridge, L. (2003). The sex peptide of Drosophila melanogaster: Female post-mating responses analyzed by using RNA interference. Proceedings of the National Academy of Sciences of the United States of America *100*, 9923-9928. 10.1073/pnas.1631635100.

1171 15. Duvall, L.B., Basrur, N.S., Molina, H., McMeniman, C.J., and Vosshall, L.B. (2017). A Peptide
1172 Signaling System that Rapidly Enforces Paternity in the Aedes aegypti Mosquito. Current
1173 Biology *27*, 3734-3742.e3735. 10.1016/j.cub.2017.10.074.
1174 16. Wolfner, M.F. (2002). The gifts that keep on giving: physiological functions and evolutionary
1175 dynamics of male seminal proteins in Drosophila. Heredity *88*, 85-93.
1176 10.1038/sj.hdy.6800017.
1177 17. Gorter, J.A., Jagadeesh, S., Gahr, C., Boonekamp, J.J., Levine, J.D., and Billeter, J.C. (2016). The
1178 nutritional and hedonic value of food modulate sexual receptivity in Drosophila melanogaster
1179 females. Sci Rep *6*, 19441. 10.1038/srep19441.
1180 18. Chen, P.S., Stumm-Zollinger, E., Aigaki, T., Balmer, J., Bienz, M., and Böhlen, P. (1988). A male
1181 accessory gland peptide that regulates reproductive behavior of female D. melanogaster. Cell
1182 *54*, 291-298. https://doi.org/10.1016/0092-8674(88)90192-4.
1183 19. Ellendersen, B.E., and von Philipsborn, A.C. (2017). Neuronal modulation of D. melanogaster
1184 sexual behaviour. Curr Opin Insect Sci *24*, 21-28. 10.1016/j.cois.2017.08.005.
1185 20. Klowden, M.J. (1999). The check is in the male: male mosquitoes affect female physiology
1186 and behavior. J Am Mosq Control Assoc *15*, 213-220.
1187 21. Manning, A. (1962). A Sperm Factor Affecting the Receptivity of Drosophila Melanogaster
1188 Females. Nature *194*, 252-253. 10.1038/194252a0.
1189 22. McCall, P.J. (2000). The biology of mosquitoes: volume 2, sensory reception and behaviour. By
1190 A.N. Clements (Wallingford, CABI Publishing, 1999). 740 pp. Hard cover £95.00 (US$175.00).
1191 ISBN 0 85199 313 3. Bulletin of Entomological Research *90*, 99-99.
1192 10.1017/S0007485300000171.
1193 23. Lung, O., Tram, U., Finnerty, C.M., Eipper-Mains, M.A., Kalb, J.M., and Wolfner, M.F. (2002).
1194 The Drosophila melanogaster seminal fluid protein Acp62F is a protease inhibitor that is toxic
1195 upon ectopic expression. Genetics *160*, 211-224.
1196 24. Pondeville, E., Maria, A., Jacques, J.C., Bourgouin, C., and Dauphin-Villemant, C. (2008).
1197 Anopheles gambiae males produce and transfer the vitellogenic steroid hormone
1198 20-hydroxyecdysone to females during mating. Proceedings of the National Academy of
1199 Sciences of the United States of America *105*, 19631-19636. 10.1073/pnas.0809264105.
1200 25. Zhang, Y.J., Zhang, N., Bu, R.T., Nässel, D.R., Gao, C.F., and Wu, S.F. (2025). A novel male
1201 accessory gland peptide reduces female post-mating receptivity in the brown planthopper.
1202 Plos Genet *21*, e1011699. 10.1371/journal.pgen.1011699.
1203 26. Saudan, P., Hauck, K., Soller, M., Choffat, Y., Ottiger, M., Sporri, M., Ding, Z., Hess, D., Gehrig,
1204 P.M., Klauser, S., et al. (2002). Ductus ejaculatorius peptide 99B (DUP99B), a novel Drosophila
1205 melanogaster sex-peptide pheromone. Eur J Biochem *269*, 989-997.
1206 10.1046/j.0014-2956.2001.02733.x.
1207 27. Herndon, L.A., and Wolfner, M.F. (1995). A Drosophila seminal fluid protein, Acp26Aa,
1208 stimulates egg laying in females for 1 day after mating. Proceedings of the National Academy
1209 of Sciences of the United States of America *92*, 10114-10118. 10.1073/pnas.92.22.10114.
1210 28. Mackay, T.F.C., Ram, K.R., and Wolfner, M.F. (2007). Sustained Post-Mating Response in
1211 Drosophila melanogaster Requires Multiple Seminal Fluid Proteins. Plos Genet *3*.
1212 10.1371/journal.pgen.0030238.
1213 29. Heifetz, Y., Vandenberg, L.N., Cohn, H.I., and Wolfner, M.F. (2005). Two cleavage products of
1214 the Drosophila accessory gland protein ovulin can independently induce ovulation.

1215 Proceedings of the National Academy of Sciences of the United States of America *102*,
1216 743-748. 10.1073/pnas.0407692102.
1217 30. Desplan, C., Gligorov, D., Sitnik, J.L., Maeda, R.K., Wolfner, M.F., and Karch, F. (2013). A Novel
1218 Function for the Hox Gene Abd-B in the Male Accessory Gland Regulates the Long-Term
1219 Female Post-Mating Response in Drosophila. Plos Genet *9*. 10.1371/journal.pgen.1003395.
1220 31. Hopkins, B.R., Angus-Henry, A., Kim, B.Y., Carlisle, J.A., Thompson, A., and Kopp, A. (2024).
1221 Decoupled evolution of the Sex Peptide gene family and Sex Peptide Receptor in
1222 Drosophilidae. Proceedings of the National Academy of Sciences of the United States of
1223 America *121*, e2312380120. 10.1073/pnas.2312380120.
1224 32. Jang, Y.-H., Chae, H.-S., and Kim, Y.-J. (2017). Female-specific myoinhibitory peptide neurons
1225 regulate mating receptivity in Drosophila melanogaster. Nature communications *8*.
1226 10.1038/s41467-017-01794-9.
1227 33. Chen, J., Zhu, P., Jin, S., Zhang, Z., Jiang, S., Li, S., Liu, S., Peng, Q., and Pan, Y. (2025). A
1228 hormone-to-neuropeptide pathway inhibits sexual receptivity in immature Drosophila
1229 females. Proceedings of the National Academy of Sciences of the United States of America
1230 *122*, e2418481122. 10.1073/pnas.2418481122.
1231 34. Avila, F.W., Sirot, L.K., LaFlamme, B.A., Rubinstein, C.D., and Wolfner, M.F. (2011). Insect
1232 seminal fluid proteins: identification and function. Annual review of entomology *56*, 21-40.
1233 10.1146/annurev-ento-120709-144823.
1234 35. Hasemeyer, M., Yapici, N., Heberlein, U., and Dickson, B.J. (2009). Sensory Neurons in the
1235 Drosophila Genital Tract Regulate Female Reproductive Behavior. Neuron *61*, 511-518.
1236 10.1016/j.neuron.2009.01.009.
1237 36. Rezával, C., Pavlou, H.J., Dornan, A.J., Chan, Y.B., Kravitz, E.A., and Goodwin, S.F. (2012).
1238 Neural circuitry underlying Drosophila female postmating behavioral responses. Current
1239 biology : CB *22*, 1155-1165. 10.1016/j.cub.2012.04.062.
1240 37. Auer, T.O., and Benton, R. (2016). Sexual circuitry in Drosophila. Curr Opin Neurobiol *38*,
1241 18-26. 10.1016/j.conb.2016.01.004.
1242 38. Lin, P.X., Peng, Y.X., Xing, J.Y., Liu, Z.Y., Guo, F.R., Thia, J.A., Gao, C.F., and Wu, S.F. (2025).
1243 Cis-regulation of the CYP6CS1 gene and its role in mediating cross-resistance in a
1244 pymetrozine-resistant strain of Nilaparvata lugens. Insect biochemistry and molecular biology
1245 *177*, 104261. 10.1016/j.ibmb.2025.104261.
1246 39. Wu, S.F., Zeng, B., Zheng, C., Mu, X.C., Zhang, Y., Hu, J., Zhang, S., Gao, C.F., and Shen, J.L.
1247 (2018). The evolution of insecticide resistance in the brown planthopper (Nilaparvata lugens
1248 Stål) of China in the period 2012-2016. Sci Rep *8*, 4586. 10.1038/s41598-018-22906-5.
1249 40. Song, X.Y., Peng, Y.X., Wang, L.X., Ye, W.N., Pei, X.G., Zhang, Y.C., Zhang, S., Gao, C.F., and Wu,
1250 S.F. (2022). Monitoring, cross-resistance, inheritance, and fitness costs of brown
1251 planthoppers, Nilaparvata lugens, resistance to pymetrozine in China. Pest management
1252 science *78*, 3980-3987. 10.1002/ps.7017.
1253 41. Ye, W.N., Li, Y., Zhang, Y.C., Liu, Z.Y., Song, X.Y., Pei, X.G., Wu, S.F., and Gao, C.F. (2024).
1254 Area-wide survey and monitoring of insecticide resistance in the brown planthopper,
1255 Nilaparvata lugens (Stål), from 2020 to 2023 in China. Pestic Biochem Physiol *205*, 106173.
1256 10.1016/j.pestbp.2024.106173.
1257 42. Tayler, T.D., Pacheco, D.A., Hergarden, A.C., Murthy, M., and Anderson, D.J. (2012). A
1258 neuropeptide circuit that coordinates sperm transfer and copulation duration in

Drosophila. Proceedings of the National Academy of Sciences *109*, 20697-20702. 10.1073/pnas.1218246109.

43. Li, H., Cheng, S., Niu, Y., Diao, T., Zhang, Q., and Zhang, W. (2025). A heart releasing neuropeptide that synchronizes brain-heart regulation during courtship behavior. bioRxiv, 2025.2003.2031.646145. 10.1101/2025.03.31.646145.

44. Tayler, T.D., Pacheco, D.A., Hergarden, A.C., Murthy, M., and Anderson, D.J. (2012). A neuropeptide circuit that coordinates sperm transfer and copulation duration in Drosophila. Proceedings of the National Academy of Sciences of the United States of America *109*, 20697-20702. 10.1073/pnas.1218246109.

45. Gospocic, J., Shields, E.J., Glastad, K.M., Lin, Y., Penick, C.A., Yan, H., Mikheyev, A.S., Linksvayer, T.A., Garcia, B.A., Berger, S.L., et al. (2017). The Neuropeptide Corazonin Controls Social Behavior and Caste Identity in Ants. Cell *170*, 748-759.e712. 10.1016/j.cell.2017.07.014.

46. Hou, Q.-L., Chen, E.-H., Jiang, H.-B., Yu, S.-F., Yang, P.-J., Liu, X.-Q., Park, Y., Wang, J.-J., and Smagghe, G. (2018). Corazonin Signaling Is Required in the Male for Sperm Transfer in the Oriental Fruit Fly Bactrocera dorsalis. Front Physiol *9*. 10.3389/fphys.2018.00660.

47. Shohat-Ophir, G., Kaun, K.R., Azanchi, R., Mohammed, H., and Heberlein, U. (2012). Sexual deprivation increases ethanol intake in Drosophila. Science *335*, 1351-1355. 10.1126/science.1215932.

48. Zer-Krispil, S., Zak, H., Shao, L., Ben-Shaanan, S., Tordjman, L., Bentzur, A., Shmueli, A., and Shohat-Ophir, G. (2018). Ejaculation Induced by the Activation of Crz Neurons Is Rewarding to Drosophila Males. Current Biology *28*, 1445-1452.e1443. 10.1016/j.cub.2018.03.039.

49. Cheng, J., Zhao, P., Zhu, L., Zhu, F., Tian, Z., Shen, Z., Liu, X., and Liu, X. (2022). Corazonin signaling modulates the synthetic activity of male accessory gland in Grapholita molesta. Int J Biol Macromol *216*, 446-455. 10.1016/j.ijbiomac.2022.07.025.

50. Yang, C.h., Belawat, P., Hafen, E., Jan, L.Y., and Jan, Y.N. (2008). Drosophila Egg-Laying Site Selection as a System to Study Simple Decision-Making Processes. Science *319*, 1679-1683. 10.1126/science.1151842.

51. Tanaka, Y., Suetsugu, Y., Yamamoto, K., Noda, H., and Shinoda, T. (2014). Transcriptome analysis of neuropeptides and G-protein coupled receptors (GPCRs) for neuropeptides in the brown planthopper Nilaparvata lugens. Peptides *53*, 125-133. 10.1016/j.peptides.2013.07.027.

52. Roller, L., Tanaka, Y., and Tanaka, S. (2003). Corazonin and corazonin-like substances in the central nervous system of the Pterygote and Apterygote insects. Cell Tissue Res *312*, 393-406. 10.1007/s00441-003-0722-4.

53. Nässel, D.R., and Zandawala, M. (2019). Recent advances in neuropeptide signaling in Drosophila, from genes to physiology and behavior. 10.7287/peerj.preprints.27515v2.

54. Kubrak, O.I., Lushchak, O.V., Zandawala, M., and Nässel, D.R. (2016). Systemic corazonin signalling modulates stress responses and metabolism in Drosophila. Open Biol *6*. 10.1098/rsob.160152.

55. Nallasivan, M.P., Singh, D.N.D., Saleh, M.S.R.S., and Soller, M. (2024). Sex-peptide targets distinct higher order processing neurons in the brain to induce the female post-mating response. eLife Sciences Publications, Ltd.

1301 56. Isaac, R.E., Li, C., Leedale, A.E., and Shirras, A.D. (2010). Drosophila male sex peptide inhibits
1302 siesta sleep and promotes locomotor activity in the post-mated female. Proc Biol Sci *277*,
1303 65-70. 10.1098/rspb.2009.1236.
1304 57. Bath, E., Bowden, S., Peters, C., Reddy, A., Tobias, J.A., Easton-Calabria, E., Seddon, N.,
1305 Goodwin, S.F., and Wigby, S. (2017). Sperm and sex peptide stimulate aggression in female
1306 Drosophila. Nat Ecol Evol *1*, 0154. 10.1038/s41559-017-0154.
1307 58. Predel, R., Neupert, S., Russell, W.K., Scheibner, O., and Nachman, R.J. (2007). Corazonin in
1308 insects. Peptides *28*, 3-10. 10.1016/j.peptides.2006.10.011.
1309 59. Boerjan, B., Verleyen, P., Huybrechts, J., Schoofs, L., and De Loof, A. (2010). In search for a
1310 common denominator for the diverse functions of arthropod corazonin: a role in the
1311 physiology of stress? Gen Comp Endocrinol *166*, 222-233. 10.1016/j.ygcen.2009.09.004.
1312 60. Veenstra, J.A. (2009). Does corazonin signal nutritional stress in insects? Insect biochemistry
1313 and molecular biology *39*, 755-762. 10.1016/j.ibmb.2009.09.008.
1314 61. Zhao, Y., Bretz, C.A., Hawksworth, S.A., Hirsh, J., and Johnson, E.C. (2010). Corazonin neurons
1315 function in sexually dimorphic circuitry that shape behavioral responses to stress in
1316 Drosophila. Plos One *5*, e9141. 10.1371/journal.pone.0009141.
1317 62. Veenstra, J.A. (1989). Isolation and structure of corazonin, a cardioactive peptide from the
1318 American cockroach. Febs Lett *250*, 231-234. 10.1016/0014-5793(89)80727-6.
1319 63. Tawfik, A.I., Tanaka, S., De Loof, A., Schoofs, L., Baggerman, G., Waelkens, E., Derua, R., Milner,
1320 Y., Yerushalmi, Y., and Pener, M.P. (1999). Identification of the gregarization-associated
1321 dark-pigmentotropin in locusts through an albino mutant. Proceedings of the National
1322 Academy of Sciences of the United States of America *96*, 7083-7087.
1323 10.1073/pnas.96.12.7083.
1324 64. Tanaka, Y., Hua, Y., Roller, L., and Tanaka, S. (2002). Corazonin reduces the spinning rate in the
1325 silkworm, Bombyx mori. J Insect Physiol *48*, 707-714. 10.1016/s0022-1910(02)00094-x.
1326 65. Kim, Y.J., Spalovská-Valachová, I., Cho, K.H., Zitnanova, I., Park, Y., Adams, M.E., and Zitnan, D.
1327 (2004). Corazonin receptor signaling in ecdysis initiation. Proceedings of the National
1328 Academy of Sciences of the United States of America *101*, 6704-6709.
1329 10.1073/pnas.0305291101.
1330 66. Imura, E., Shimada-Niwa, Y., Nishimura, T., Hückesfeld, S., Schlegel, P., Ohhara, Y., Kondo, S.,
1331 Tanimoto, H., Cardona, A., Pankratz, M.J., and Niwa, R. (2020). The Corazonin-PTTH Neuronal
1332 Axis Controls Systemic Body Growth by Regulating Basal Ecdysteroid Biosynthesis in
1333 Drosophila melanogaster. Current biology : CB *30*, 2156-2165.e2155.
1334 10.1016/j.cub.2020.03.050.
1335 67. Zandawala, M., Nguyen, T., Balanya Segura, M., Johard, H.A.D., Amcoff, M., Wegener, C.,
1336 Paluzzi, J.P., and Nassel, D.R. (2021). A neuroendocrine pathway modulating osmotic stress in
1337 Drosophila. Plos Genet *17*, e1009425. 10.1371/journal.pgen.1009425.
1338 68. Xi, J., Hamanaka, Y., and Shiga, S. (2025). Corazonin mediates photoperiodically induced
1339 diapause in the bean bug Riptortus pedestris. J Exp Biol *228*. 10.1242/jeb.250528.
1340 69. Wu, S.-F., Jv, X.-M., Li, J., Xu, G.-J., Cai, X.-Y., and Gao, C.-F. (2017). Pharmacological
1341 characterisation and functional roles for egg-laying of a β-adrenergic-like octopamine
1342 receptor in the brown planthopper Nilaparvata lugens. Insect biochemistry and molecular
1343 biology *87*, 55-64. https://doi.org/10.1016/j.ibmb.2017.06.008.

1344 70. Krogh, A., Larsson, B., von Heijne, G., and Sonnhammer, E.L. (2001). Predicting
1345 transmembrane protein topology with a hidden Markov model: application to complete
1346 genomes. J Mol Biol *305*, 567-580. 10.1006/jmbi.2000.4315.
1347 71. Livak, K.J., and Schmittgen, T.D. (2001). Analysis of Relative Gene Expression Data Using
1348 Real-Time Quantitative PCR and the 2−ΔΔCT Method. Methods *25*, 402-408.
1349 https://doi.org/10.1006/meth.2001.1262.
1350 72. Sun, H., Bu, L.-A., Su, S.-C., Guo, D., Gao, C.-F., and Wu, S.-F. (2023). Knockout of the odorant
1351 receptor co-receptor, orco, impairs feeding, mating and egg-laying behavior in the fall
1352 armyworm Spodoptera frugiperda. Insect biochemistry and molecular biology *152*.
1353 10.1016/j.ibmb.2022.103889.
1354 73. Zhang, Y.C., Gao, Y., Ye, W.N., Peng, Y.X., Zhu, K.Y., and Gao, C.F. (2023). CRISPR/Cas9-mediated
1355 knockout of NlCYP6CS1 gene reveals its role in detoxification of insecticides in Nilaparvata
1356 lugens (Hemiptera: Delphacidae). Pest management science *79*, 2239-2246.
1357 10.1002/ps.7404.
1358 74. Yan, H., Opachaloemphan, C., Carmona-Aldana, F., Mancini, G., Mlejnek, J., Descostes, N.,
1359 Sieriebriennikov, B., Leibholz, A., Zhou, X., Ding, L., et al. (2022). Insulin signaling in the
1360 long-lived reproductive caste of ants. Science *377*, 1092-1099. 10.1126/science.abm8767.

1361

1362